Studies on chemical valence speciation analyses

of trace sulfur and tin in glass

Yoshitaka Saijo

2022

Contents

Atomic Emission Spectrometry after the Decomposition

Utilizing Ascorbic Acid **56**

Chapter4

Speciation Analysis of Tin at the Tin Side of Float Glass by

Solvent Extraction Combined with a Stepwise Etching

Technique **86**

General Introduction

Glass is a versatile material used in various industries and has a wide range of compositions. New glass compositions are constantly being developed for various applications. In addition to the major components, trace elements affect various glass properties, such as transparency[1], color[2], photoluminescence[3], crystallization[4], and manufacturing properties[5–7]. Multivalent elements are added as trace elements to glass to adjust its properties. Furthermore, during mass production, several multivalent elements can be mixed into glass as impurities derived from the raw materials or materials used during the manufacturing process. They also affect the glass properties listed above. The total concentration of multivalent elements and the concentration of each valence of the element affect the glass properties. Therefore, determining the concentration of each valence of multivalent elements in glass is important for adjusting its properties, and reliable methods for achieving this outcome are required. The methods should be quantitative, valence-selective, and highly sensitive because of the low concentrations of the target elements. Furthermore, these methods must be performed at mass-production sites to optimize the properties of the actual product glass. These methods should be routinely executable using the equipment and apparatus commonly used in laboratories.

Examples of multivalent elements in glass include S, Ti, V, Cr, Mn, Fe, Co, Ni, Cu, As, Se, Mo, Ag, Sn, Sb, Ce, Pr, Nd, Sm, Eu, and Er. These are typically added in the form of oxides or salts. S is added to the glass as a fining[8–10] and coloring agent[11–13]. As, Sb, Ce, and Sn are also used as fining agents[14]. As and Sb are currently avoided because of the legislation that regulates the use of hazardous elements[15–17]. The fining agents were replaced with Sn[17]. Fe is a common element added to glass and functions as a coloring agent[14,18–20]. Ti, V, Cr, Mn, Co, Ni, Cu, Se, Mo, Pr, Nd, Sm, Eu, and Er are also typically used as coloring agents[14]. The fining process is based on a

reduction–oxidation reaction, and the coloration depends on the concentration of each multivalent element. Examples of multivalent elements mixed into glass as impurities derived from raw materials or materials used in manufacturing processes are S, Ti, Cr, Mn, Fe, Ni, Mo, Sn, and Pt. Fe is an unavoidable impurity in raw materials, particularly in silica sand. Mo is used as an electric melting electrode for raw glass materials, and part of it melts and mixes into glass[21,22]. Sn has been used in the float method, which is a mass-production technique implemented to form plate-shaped glass[23]. In this method, molten glass is suspended over molten tin, which penetrates the glass surface in contact with it at the glass–tin interface. Pt was used as a glass melting container, and part of it was melted and mixed with the glass[24–26]. Multivalent elements mixed into glass remain there at multiple valences and affect the glass properties. Hence, it is necessary to determine the concentration of each valence of multivalent elements in the glass.

The methods for determining the valence ratios and concentrations of multivalent elements can typically be divided into physical and wet chemical analyses. Examples of physical analysis methods include Mössbauer spectroscopy[27,28], X-ray absorption fine structure (XAFS) analysis[29–32], high-resolution X-ray fluorescence (HR-XRF) analysis[33–35], electron probe microanalysis (EPMA)[30,36,37], Raman spectroscopy[38,39], electron spin resonance (ESR) spectroscopy [19,40,41], transmission electron microscopy–electron energy loss spectroscopy (TEM-EELS)[42], and X-ray photoelectron spectroscopy (XPS)[43]. A common advantage of physical analysis is elemental selectivity, as the interference from other elements is small or negligible. However, the common disadvantages are the high cost of the equipment and limitations associated with its use.

Examples of chemical analyses include colorimetry for Fe[44–47] and Sn in glass[48], oxidimetry–colorimetry for Fe in glass[49,50] and rock[51], titration for Sn in glass[52], a hydrosulfide volatilization method for S in rock[53,54] and glass[55,56], ion chromatography and inductively coupled plasma atomic emission spectroscopy (ICP-AES) for Sb in glass[57], and reversed-phase

liquid chromatography for As in soil[58]. The common advantages of wet chemical analysis are high

precision, low detection limit, and low cost. These features are useful for the routine analysis required

in this study. However, wet chemical analysis for the valence analysis of multivalent elements in glass

poses several challenges. First, the decomposition of the glass sample is necessary, which can cause a

change in the valence of the target elements. Second, the separation of multiple valence states is

required. Finally, highly sensitive determination is required owing to the low concentrations of

multivalent elements.

In this study, S and Sn were selected as multivalent elements in glass. This is because despite them

being important additive elements in glass, valence analysis methods that can be performed routinely

with commonly used equipment and apparatus have not yet been established. Examples of sulfur

valence analysis in glass include EPMA[30,36], Raman spectroscopy[38,39], HR-XRF[33,34],

XAFS[29,30,32], and hydrogen sulfide volatilization[55,56]. However, these methods pose certain

challenges. EPMA and XAFS have the disadvantage of beam damage, which leads to a change in

sulfur valence during the analysis. Furthermore, the use of synchrotron radiation facilities for XAFS

renders its routine use challenging. Raman spectroscopy cannot quantitatively determine trace sulfides

and sulfates. HR-XRF has a low signal-to-noise ratio owing to its two-crystal system, and its analysis

is time-consuming. A hydrogen sulfide volatilization method can determine the sulfide content in

glass; however, the total sulfur content needs to be determined using different experiments. Examples

of tin valence analysis in glass include Mössbauer spectroscopy[33–35], HR-XRF[34,35], XAFS[32],

titration[52], and spectrophotometric methods[48]. However, these methods have several

disadvantageous that limit their application. Mössbauer spectroscopy requires a radiation-controlled

area and an accurate measurement of the Debye temperature of each target ion. The drawbacks of HR-

XRF and XAFS have been described previously. Titration and spectrophotometric methods are

examples of chemical analyses that have favorable features for the routine analysis required in this

study. However, these studies[48,52] did not consider the effects of other multivalent elements in the glass. Sn and other multivalent elements undergo redox reactions during decomposition, changing the ratio of $Sn^{2+}:Sn^{4+}$ from that of glass. Fe is a typical multivalent element that is always present as a raw material in industrially manufactured glass or as an impurity derived from the material used during the manufacturing process, and it undergoes redox reaction with Sn. Therefore, previous methods, which target actual mass-produced glass products, cannot be used in this study.

The purpose of this thesis is to develop, describe, demonstrate, and validate new methods for determining the concentration of each valence state of S and Sn in glass to overcome the aforementioned challenges, such as the decomposition of glass without changes in the valences of the target elements, separation of multiple valence states, and developing a method for highly sensitive determination of valence states. Soda lime silicate glass was selected as the base composition as it accounts for more than 80% of the glass market[59]. The methods studied in this thesis were designed and developed for routine analyses in ordinary laboratories. These methods can help improve the properties and design of high-performance glass. Ultimately, utilizing these methods improves the mass production yield, thereby saving energy and reducing CO_2 emissions.

Summary of each chapter

Chapter1:

  A simple, rapid, and accurate method to determine the concentration of sulfur in soda lime silicate glass was developed as a basic method for the development of valence analysis methods. This method requires a smaller number of samples and takes less time for the analysis than conventional methods. The samples of glass were decomposed using hydrofluoric acid, perchloric acid, and an oxidizing agent. For the amber glass samples, the oxidizing agent used was potassium permanganate. The decomposed solution was diluted with perchloric acid. The solution was passed through an alumina column to enable sulfur adsorption on the column. To desorb sulfur from the column, diluted ammonia was passed through it after rinsing it with diluted perchloric acid. ICP-AES was used to determine the concentration of sulfur in the ammonia eluent.

Chapter2:

  A new method to determine the concentrations of sulfide and sulfate in glass was developed. This method consists of decomposition of a glass material and the separation and determination of sulfide and sulfate. Hydrochloric acid and hydrofluoric acid decomposed the material in a vessel. The vessel was combined with a series of traps. Hydrogen peroxide and sodium hydroxide in the traps absorbed hydrogen sulfide that volatilized during decomposition. This method allowed for the determination of sulfate remaining in the vessel and the trapped sulfide, respectively. The method was tested on two glass reference materials with commonly used testing equipment. The sums of sulfide and sulfate were within the range of each certified value. The average valences of sulfur, which were calculated from the quantities of sulfide and sulfate, were in good agreement with the average valences of sulfur obtained by wavelength-dispersive X-ray fluorescence spectrometric analysis.

Chapter3:

A new method to determine the concentrations of Sn^{2+} and Sn^{4+} in soda lime glass containing iron oxide was developed. A mixture of ascorbic acid, hydrochloric acid, and hydrofluoric acid was used to decompose the sample in a vessel with nitrogen flow. Ascorbic acid functioned as a reductant for Fe^{3+}. Subsequently, the Sn^{2+} were separated as a diethyldithiocarbamate complex. Furthermore, an inductively coupled plasma atomic emission spectroscopy was used to determine the concentrations of Sn^{4+} and total Sn, from which the concentration of Sn^{2+} can be calculated. The results were validated by comparing ratios of Sn^{2+} to total Sn to results obtained using Mössbauer spectroscopy.

Chapter4:

A quantitative analysis method for determining the concentrations of total Sn and Sn^{4+} that penetrate the surface of a float glass that was in contact with the molten tin was developed by applying the method developed in chapter 3. This method consists of three steps: stepwise etching of a glass sample, separation of tin species, and determination of the total Sn and Sn^{4+} concentrations. The concentration of Sn^{2+} and the ratio of Sn^{2+} to total Sn (Sn redox) were calculated from the total Sn and Sn^{4+} concentrations. This method provides quantitative depth profiles of the total Sn, Sn^{4+}, Sn^{2+}, and the Sn redox. When the total Sn concentration (as SnO_2) is greater than 0.2 mass%, this method has the finest depth resolution, 0.1 μm, as compared with other techniques. Moreover, it can be implemented in the laboratory because it requires only commonly used apparatus and equipment. The proposed method can be used to obtain detailed information about tin penetrating the float glass, and thereby strongly contributes to the float process for producing high-quality glass.

References

[1]   Y. Arai, M. Inoue, K. Ishikawa, T. Yokote, Y. Kondo, K. Mori, Evolution of the glass light

        guide plate and its peripheral technologies for large size TV application, 2017.

        https://doi.org/10.1002/sdtp.11964.

[2]   W.A. Wely, Coloured Glasses, Society of Glass Technology, Sheffiled, 1981.

[3]   M.R. Cicconi, A. Veber, D. de Ligny, J. Rocherullé, R. Lebullenger, F. Tessier, Chemical

        tunability of europium emission in phosphate glasses, Journal of Luminescence. 183 (2017).

        https://doi.org/10.1016/j.jlumin.2016.11.019.

[4]   G.H. Beall, Design and properties of glass-ceramics, Annual Review of Materials Science. 22

        (1992). https://doi.org/10.1146/annurev.ms.22.080192.000515.

[5]   D.B. Dingwell, Redox viscometry of some Fe-bearing silicate melts, American Mineralogist.

        76 (1991).

[6]   D.B. Dingwell, Shear viscosities of ferrosilicate liquids, American Mineralogist. 74 (1989).

[7]   H. Tokunaga, Thermal conductivity measurement of glass melts and its applications, NEW

        GLASS. 34 (2019) 14–18.

[8]   R.G.C. Beerkens, Sulphate decomposition and sulphur chemistry in glass melting processes,

        Glass Technology. 46 (2005) 39–46.

[9]   R.G.C. Beerkens, K. Kahl, Chemistry of sulphur in soda-lime-silica glass melts, Physics and

        Chemistry of Glasses. 43 (2002) 189–198.

[10]   M. CABLE, Kinetics and Mechanisms of Fining Glasses, Journal of the American Ceramic

        Society. 49 (1966). https://doi.org/10.1111/j.1151-2916.1966.tb15412.x.

[11]   F.L. Harding, Effect of base glass composition on amber colour, Glass Technology. 13 (1972)

        43–49.   https://pascal-

        francis.inist.fr/vibad/index.php?action=getRecordDetail&idt=PASCAL7388000957

(accessed November 26, 2021).

[12]   D. Brown, R.W. Douglas, "Carbon-suiphur" amber glass, Glass Technology. 6 (1965) 190–
          196.

[13]   R.G.C. Beerkens, Amber chromophore formation in sulphur- and iron-containing soda-lime-
          silica   glasses,   Glass   Science   and   Technology.   76   (2003)   166–175.
          https://research.tue.nl/en/publications/amber-chromophore-formation-in-sulphur-and-iron-
          containing-soda-l (accessed November 26, 2021).

[14]   J.D. Musgraves, J. Hu, L. Calvez, eds., Handbook of glass, Springer Nature Switzerland AG,
          Gewerbestrasse, 2019. https://doi.org/10.1007/978-3-319-93728-1.

[15]   ECHA-Substance   Information-Diarsenic   trioxide,   https://echa.europa.eu/substance-
          information/-/substanceinfo/100.014.075 (accessed May 11, 2022).

[16]   ECHA- Substance Information-Diarsenic pentaoxide, https://echa.europa.eu/substance-
          information/-/substanceinfo/100.013.743 (accessed May 11, 2022).

[17]   A. Ellison, I.A. Cornejo, Glass Substrates for Liquid Crystal Displays, International Journal of
          Applied Glass Science. 1 (2010) 87–103. https://doi.org/10.1111/j.2041-1294.2010.00009.x.

[18]   D. Ehrt, M. Leister, A. Matthai, Polyvalent elements iron, tin and titanium in silicate, phosphate
          and fluoride glasses and melts, Physics and Chemistry of Glasses. 42 (2001).

[19]   P.S. Danielson, J.W.H. Schreurs, Optical and EPR absorptions of iron in alkaline earth
          aluminosilicate   glasses,   Journal   of   Non-Crystalline   Solids.   38–39   (1980).
          https://doi.org/10.1016/0022-3093(80)90414-7.

[20]   H. Hijiya, Consideration on the structure of Fe^{2+} in system, NEW GLASS. 34 (2019) 14–17.

[21]   K. Takahashi, Y. Miura, Electrochemical behavior of glass melts, Journal of Non-Crystalline
          Solids. 95–96 (1987). https://doi.org/10.1016/S0022-3093(87)80104-7.

[22]   M. Yamamoto, K. Sakai, R. Akagi, Þ. Sakai, Þ. Hiroshi, Y. Þand, T. Maekawaþ,

Electrochemical Corrosion of Molybdenum Electrodes in an Aluminosilicate Glass Melt Containing Antimony, Journal of the Ceramic Society of Japan. 112 (2004) 179–183. https://doi.org/10.2109/jcersj.112.179.

[23] L.A.B. Pilkington, The float glass process, Proceeding of the Royal Society A, 314 (1969) 1–25. https://doi.org/10.1098/rspa.1969.0212.

[24] J.H. Campbell, E.P. Wallerstein, J.S. Hayden, D.L. Sapak, D.E. Warrington, A.J. Marker, Effects of melting conditions on platinum-inclusion content in phosphate laser glasses, Glass Science and Technology Frankfurt. 68 (1995).

[25] J.H. Campbell, E.P. Wallerstein, H. Toratani, H.E. Meissher, S. Nakajima, T.S. Izumitani, Effects of process gas environment on platinum-inclusion density and dissolution rate in phosphate laser glasses, Glass Science and Technology Frankfurt. 68 (1995).

[26] M. Yamamoto, R. Akiyama, Platinum and Rhodium Dissolution Behavior in Non-alkaline Glass Melt, Reports of the Research Laboratory, Asahi Glass Co. 56 (2006) 7–11.

[27] J.A. Johnson, C.E. Johnson, Mössbauer spectroscopy as a probe of silicate glasses, Journal of Physics Condensed Matter. 17 (2005). https://doi.org/10.1088/0953-8984/17/8/R01.

[28] H.L. Zhang, E. Cottrell, P.A. Solheid, K.A. Kelley, M.M. Hirschmann, Determination of $Fe^{3+}/\Sigma Fe$ of XANES basaltic glass standards by Mössbauer spectroscopy and its application to the oxidation state of iron in MORB, Chemical Geology. 479 (2018) 166–175. https://doi.org/10.1016/j.chemgeo.2018.01.006.

[29] L. Backnaes, J. Stelling, H. Behrens, J. Goettlicher, S. Mangold, O. Verheijen, R.G.C. Beerkens, J. Deubener, Dissolution mechanisms of tetravalent sulphur in silicate melts: Evidences from sulphur K edge XANES studies on glasses, in: Journal of the American Ceramic Society, 2008. https://doi.org/10.1111/j.1551-2916.2007.02044.x.

[30] K. Klimm, S.C. Kohn, L.A. O'Dell, R.E. Botcharnikov, M.E. Smith, The dissolution

mechanism of sulphur in hydrous silicate melts. I: Assessment of analytical techniques in determining the sulphur speciation in iron-free to iron-poor glasses, Chemical Geology. 322–323 (2012) 237–249. https://doi.org/10.1016/j.chemgeo.2012.04.027.

[31]   F. Farges, Y. Lefrère, S. Rossano, A. Berthereau, G. Calas, G.E. Brown, The effect of redox state on the local structural environment of iron in silicate glasses: A combined XAFS spectroscopy, molecular dynamics, and bond valence study, Journal of Non-Crystalline Solids. 344 (2004) 176–188. https://doi.org/10.1016/j.jnoncrysol.2004.07.050.

[32]   A.M. Flank, P. Lagarde, J. Jupille, H. Montigaud, Redox profile of the glass surface, Journal of   Non-Crystalline   Solids.   357   (2011)   3200–3206. https://doi.org/10.1016/j.jnoncrysol.2011.03.046.

[33]   A. Faessler, M. Goehring, Röntgenspektrum und Bindungszustand - Die Kα-Fluoreszenzstrahlung   des   Schwefels,   Naturwissenschaften.   39   (1952). https://doi.org/10.1007/BF00589801.

[34]   Y. Gohshi, O. Hirao, I. Suzuki, Chemical State Analyses of Sulfur, Chromium and Tin by High Resolution   X-Ray   Spectrometry,   Advances   in   X-Ray   Analysis.   18   (1974). https://doi.org/10.1154/s0376030800006911.

[35]   H. Masuda, Y. Fukumoto, K. Morinaga, Sn^{2+}/Sn^{4+} Redox Equilibrium in the Oxide Glasses, Interdisciplinary Graduate School of Engineering Sciences, Kyushu University. 14 (1992) 173–179. https://doi.org/10.15017/17267.

[36]   M.R. Carroll, M.J. Rutherford, Sulfur speciation in hydrous experimental glasses of varying oxydation states: Results from measured wavelength shifts of sulfur X-rays, American Mineralogist. 73 (1988).

[37]   X. Llovet, A. Moy, P.T. Pinard, J.H. Fournelle, Electron probe microanalysis: A review of recent developments and applications in materials science and engineering, Progress in

Materials Science. 116 (2021). https://doi.org/10.1016/j.pmatsci.2020.100673.

[38] K. Klimm, R.E. Botcharnikov, The determination of sulfate and sulfide species in hydrous silicate glasses using Raman spectroscopy, American Mineralogist. 95 (2010) 1574–1579. https://doi.org/10.2138/am.2010.3590.

[39] M. Wilke, K. Klimm, S.C. Kohn, Spectroscopic studies on sulfur speciation in synthetic and natural glasses, Reviews in Mineralogy and Geochemistry. 73 (2011) 41–78. https://doi.org/10.2138/rmg.2011.73.3.

[40] N. Pathak, S.K. Gupta, K. Sanyal, M. Kumar, R.M. Kadam, V. Natarajan, Photoluminescence and EPR studies on Fe^{3+} doped $ZnAl_2O_4$: An evidence for local site swapping of Fe^{3+} and formation of inverse and normal phase, Dalton Transactions. 43 (2014) 9313–9323. https://doi.org/10.1039/c4dt00741g.

[41] V. Vercamer, G. Lelong, H. Hijiya, Y. Kondo, L. Galoisy, G. Calas, Diluted Fe^{3+} in silicate glasses: Structural effects of Fe-redox state and matrix composition. An optical absorption and X-band/Q-band EPR study, Journal of Non-Crystalline Solids. 428 (2015). https://doi.org/10.1016/j.jnoncrysol.2015.08.010.

[42] W. Xiang, H. Gao, L. Ma, X. Ma, Y. Huang, L. Pei, X. Liang, Valence state control and third-order nonlinear optical properties of copper embedded in sodium borosilicate glass, ACS Applied Materials and Interfaces. 7 (2015). https://doi.org/10.1021/acsami.5b00218.

[43] W. Cao, Z. Zhou, C. Li, Q. Wang, Y. Huang, S. Shen, Different hydrothermal corrosion results between two sides of sodalime float glass and the possible corrosion mechanism, Ceramics International. 47 (2021) 1807–1818. https://doi.org/10.1016/j.ceramint.2020.09.007.

[44] D.G. Karraker, Ferrous/Ferric Ratio in DWPF Glass: Chemical and [57]Fe Mössbauer Determinations, Advanced Ceramic Materials. 3 (1988). https://doi.org/10.1111/j.1551-2916.1988.tb00230.x.

[45] D.R.J. Jones, W.C. ansheski, D.S. Goldman, Spectrophotometric Determination of Reduced and Total Iron in Glass with 1,10-Phenanthroline, Analytical Chemistry. 53 (1981) 923–924. https://doi.org/10.1021/ac00229a049.

[46] E.W. Baumann, Colorimetric determination of iron(II) and iron(III) in glass, Analyst. 117 (1992). https://doi.org/10.1039/an9921700913.

[47] O. Corumluoglu, E. Guadagnino, Determination of ferrous iron and total iron in glass by a colorimetric method, Glass Technology. 40 (1999) 24–28.

[48] R. Pyare, P. Nath, Simple and rapid spectrophotometric method for the determination of Tin(II) in binary alkali silicate glasses, Analyst. 110 (1985) 1321–1323. https://doi.org/10.1039/AN9851001321.

[49] P. Close, H.M. Shepherd, C.H. Drummond, Determination of Several Valences of Iron, Arsenic and Antimony, and Selenium in Glass, Journal of the American Ceramic Society. 41 (1958). https://doi.org/10.1111/j.1151-2916.1958.tb12894.x.

[50] W.D. Johnston, Oxidation-Reduction Equilibria in Iron-Containing Glass, Journal of the American Ceramic Society. 47 (1964). https://doi.org/10.1111/j.1151-2916.1964.tb14392.x.

[51] J.E. Amonette, J. Matyáš, Determination of ferrous and total iron in refractory spinels, Analytica Chimica Acta. 910 (2016) 25–35. https://doi.org/10.1016/j.aca.2015.12.024.

[52] J.S. Sieger, Chemical characteristics of float glass surfaces, Journal of Non-Crystalline Solids. 19 (1975) 213–220. https://doi.org/10.1016/0022-3093(75)90086-1.

[53] S. Nagashima, M. Yoshida, T. Ozawa, The Determination of Sulfide- and Sulfate-Sulfur in Igneous Rocks with Tin(II)-Strong Phosphoric Acid and Strong Phosphoric Acid, Bull Chem Soc Jpn. 45 (1972). https://doi.org/10.1246/bcsj.45.3446.

[54] Y. Arikawa, T. Ozawa, I. Iwasaki, Determination of total-sulfur in igneous rocks with tin(II)-strong phosphoric acid, BUNSEKI KAGAKU. 21 (1972) 920–924.

https://doi.org/10.2116/bunsekikagaku.21.920.

[55]   T. Yarita, A. Masui, M. Noshiro, Analysis of total- and sulfide- sulfur in silicate glasses by using strong phosphoric acid in combination with ion chromatography, Research Report of Asahi Glass Co., Ltd. 37 (1987) 37–42.

[56]   M. Kawamoto, M. Kagaya, R. Akiyama, Selective determination of trace amounts of total and sulfate-sulfur in glasses, Research Report of Asahi Glass Co., Ltd. 48 (1998) 11–19.

[57]   R. Akiyama, A. Takenaka, M. Sugizaki, Determination of Antimonic(III) and Antimonic(V) in Glasses by Ion Chromatography/Inductively Coupled Plasma Atomic Emission Spectrometry, Reports of the Research Laboratory, Asahi Glass Co. 44 (1994) 13–18.

[58]   I. Ali, C.K. Jain, Advances in arsenic speciation techniques, International Journal of Environmental Analytical Chemistry. 84 (2004). https://doi.org/10.1080/03067310410001729637.

[59]   Green Rhino Energy: Value Chain Activity: Manufacturing Solar Glass, (n.d.). http://www.greenrhinoenergy. com/solar/industry/ind_15_solarglass.php (accessed May 11, 2022).
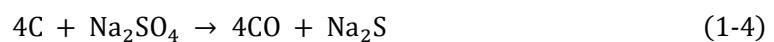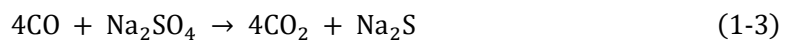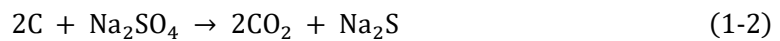
Chapter1

Determination of Total Sulfur in Soda Lime Silicate Glass by Inductively Coupled Plasma Atomic Emission Spectroscopy following Separation using an Alumina Column

1.1 Introduction

Soda lime silicate glass is the most widely used glass in the world and is the leader in the world's glass market[1]. The industrial production of glass involves batch preparation, melting, fining, refining, forming, annealing, and post processes[2]. To obtain a high-quality glass product, the number of bubbles remaining in the final product should be reduced. Fining and refining are, therefore, important in the industrial production of glass. The fining agents reduce the bubbles in the glass. One of the commonly used fining agents in the production of soda lime silicate glass is sodium sulfate (Na_2SO_4). The melting, fining, and refining reactions of soda lime silicate glass were investigated[3–10]. In oxidized melts, the main sulfate fining mechanism is thermal sulfate decomposition. It typically occurs between 1430 and 1480 °C as follows:

$$Na_2SO_4 \rightarrow Na_2O + SO_2 + \frac{1}{2}O_2 \tag{1-1}$$
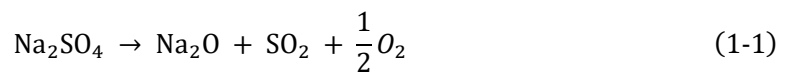
In reduced melts, which contain cokes, CO, and organic contaminants, some sulfates react to produce sulfides as follows:

$$2C + Na_2SO_4 \rightarrow 2CO_2 + Na_2S \tag{1-2}$$

$$4CO + Na_2SO_4 \rightarrow 4CO_2 + Na_2S \tag{1-3}$$

$$4C + Na_2SO_4 \rightarrow 4CO + Na_2S \tag{1-4}$$

The sulfide formation typically occurs between 700 and 800 °C, and the formed sulfides react with the remaining sulfates. Fining typically occurs between 1000 and 1350 °C as follows:

$$S^{2-} + 3SO_4^{2-} \rightarrow 4SO_2 + 4O^{2-} \tag{1-5}$$
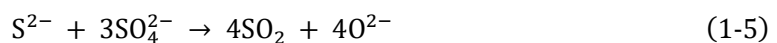
During annealing, which follows fining, fining gases such as O_2 and SO_2 are chemically absorbed into the melt, and the process is called refining. Fining and refining reduce the number of bubbles in the final product.

Determining the quantity of sulfur in the final product is important to understand the fining and refining reactions. Sulfur is said to be present in glass mainly as sulfate and sulfide[11,12]. The total quantity of sulfur, consisting of sulfate and sulfide, also has to be determined, because sulfides can remain in a final product, such as amber glass[7,13].

Several methods are already available to determine the quantity of sulfur in glass. These methods can be categorized into two types. One type decomposes the glass samples to determine the sulfur quantity in the decomposed solutions. An example of this type is the gravimetric analysis of barium sulfate[14]. The other type expels sulfur in the form of hydrogen sulfide and determines the sulfur quantity in the sample by trapping. These methods include distilled separation – methylene blue spectrophotometric method[15,16], Tin(II)-strong phosphoric acid decomposition - iodometric titration[17] , Tin(II)-strong phosphoric acid decomposition – ion chromatography[18] , reduction-distillation - hydroxymercuribenzoate titration[19] , hydrophosphorous acid – hydroiodic acid reduction[20] and sodium iodide – hydroiodic acid – hypophosphorous acid reduction[21]. However, these methods require technical skills and a large number of samples. Some methods even require special apparatuses to decompose glass samples and take a long time for the analysis. For example, the conventional gravimetric method requires a 3 g sample and at least two days for the analysis. The sodium iodide – hydroiodic acid – hypophosphorous acid reduction requires a special reduction–distillation apparatus solely to determine the sulfur quantity in the samples. This strong reduction is unsafe because the samples have to be heated in a closed flask. Isotope dilution high-resolution inductively coupled plasma mass spectrometry (ICP-MS) equipped with a flow injection system[22] is a simple and accurate method. It can determine even low levels of sulfur using only a small number

of samples but requires high-resolution ICP-MS, and thus is still not used widely. X-ray fluorescence is used in the daily measurements at glass production sites[23]. However, it requires standard materials with accurate quantities of sulfur that require calibration through other methods.

A simple, rapid, and accurate method is, therefore, required to determine the sulfur quantity in soda lime silicate glass using a smaller number of glass samples. The use of commonly used equipment to decompose the glass samples and determine their sulfur quantity is preferable. Many elements in glass are determined using decomposition methods[24].

Separating the sulfur before determining its quantity is also preferable. The sulfur separation prevents interference by glass matrix elements and improves the sensitivity of the sulfur quantity determination. Chromatographic separation using an alumina column with the gravimetric analysis of barium sulfate was used to determine the sulfur quantity in iron and steel[25]. This separation procedure was simple and rapid. However, a high blank value of sulfur (approximately 50 μg/g) was observed owing to the large alumina column and the large amount of reagents used. We developed our method by improving the method already available to reduce the blank value of sulfur. In our method, the glass samples were decomposed using hydrofluoric acid, perchloric acid, and an oxidizing agent, and thereafter the sulfur in the glass matrix elements were separated using a small high-purity alumina column. The separation procedure, which is simple and speedy, can simultaneously treat up to 10 samples.

The method we propose determines the sulfur content of glass samples containing sulfide. An oxidizing agent has to be added to the glass samples in the decomposition procedure. In the absence of an oxidizing agent, sulfides evaporate in the form of hydrogen sulfide during the sample decomposition. Br_2 is a widely used oxidizing agent[24]. However, to determine the sulfur content in glass using Br_2, additional apparatuses are required, and the decomposing reaction with cold water has to be slow. In this study, hydrogen peroxide and potassium permanganate were examined for their

16

suitability as oxidizing agents that would reduce the decomposition time of the samples. Potassium permanganate is a typical oxidizing agent used to determine the arsenic content in glass. During the decomposition of the glass samples, potassium permanganate oxidizes trivalent arsenic to form pentavalent arsenic. Potassium permanganate prevents the evaporation of trivalent arsenic during the decomposition of the samples[24]. We could confirm through this study that potassium permanganate is required to determine the total quantity of sulfur in amber glass to ensure that the determined value of sulfur is not lower than its certified value.

Inductively coupled plasma atomic emission spectroscopy (ICP-AES) was used to determine the sulfur quantity in the samples. ICP-AES, which is used widely, requires one hour for the process, which includes the time taken for equipment setting up and shutting down, standard solution measurements, and calculations performed to determine the quantity of sulfur in the samples.

1.2 Experimental

1.2.1 Materials

Three certified reference soda lime silicate glass samples were used in the experiment: the three glass types were R-1 (Japan Standard Sample Committee, Tokyo, Japan), SGT10 (Society of Glass Technology, Sheffield, United Kingdom), and SGT11 (Society of Glass Technology, Sheffield, United Kingdom). Table 1-1 lists the compositions of the three types of glass. R-1, SGT10, and SGT11 represent clear, amber, and green glass, respectively. Values in parentheses for SO_3 indicate 95 % confidence intervals. All elements are listed in the form of oxides with the maximum valence of each element, regardless of the real valence, following the conventions for describing the composition of oxide glass. For example, iron (Fe) is contained in glass materials as ferrous (Fe^{2+}) and ferric (Fe^{3+}) but listed as Fe_2O_3. Sulfur (S) is contained in glass materials as sulfide (S^{2-}) and sulfate (S^{6+}) but listed as SO_3.

Table 1-1 Certified mass fractions of glass reference materials

	Certified mass fractions (mass%)		
	R-1	SGT10	SGT11
	(Clear)	(Amber)	(Green)
SiO_2	72.2	72.7	70.7
Al_2O_3	1.75	1.62	1.83
Na_2O	13.8	12.2	13.6
K_2O	0.84	0.35	0.69
MgO	4.01	1.81	2.14
CaO	6.72	10.7	10.3
BaO	-	0.02	0.003
Fe_2O_3	0.08	0.33	0.344
TiO_2	0.03	0.097	0.068
Cr_2O_3	-	0.02	0.205
SO_3	**0.20** (0.193-0.204)	**0.05** (0.043-0.058)	**0.06** (0.055-0.069)

1.2.2 Apparatus

A 100 mL polytetrafluoroethylene (PTFE) dish was used as the decomposition container. An alumina column, InterSep AL-N Al_2O_3 500 mg/2 mL (GL Sciences Inc., Tokyo, Japan), placed on a vacuum filtration kit (GL Sciences Inc., Tokyo, Japan) was used to separate the sulfur in the samples. An inductively coupled plasma atomic emission spectrometer, SPS5520 (Hitachi High-Tech Corporation, Tokyo, Japan) was used to determine the sulfur quantity and other glass matrix elements

in the glass samples. An agate mortar and pestle were used to grind the samples. A 50 mL volumetric flask and a 100 mL volumetric flask were used.

1.2.3 Regents and chemicals

Hydrofluoric acid (50 mass%), perchloric acid (60 mass%), ammonia solution (25 mass%) of atomic absorption spectrometry grade (Kanto Chemical Co., Inc., Tokyo, Japan), hydrogen peroxide (30 mass%) of special grade (Kanto Chemical Co., Inc., Tokyo, Japan), and 0.1 mol/L of the potassium permanganate solution of reagent grade (Kanto Chemical Co., Inc., Tokyo, Japan) were used. The standard solutions used for the ICP-AES analysis were sulfate ion standard solution (1 g SO_4^{2-} /L) of ion chromatography grade (Kanto Chemical Co., Inc., Tokyo, Japan), aluminum standard solution (1 g Al/L), sodium standard solution (1 g Na/L), potassium standard solution (1 g K/L), magnesium standard solution (1 g Mg/L), calcium standard solution (1 g Ca/L), iron standard solution (1 g Fe/L), titanium standard solution (1 g Ti/L), and chromium standard solution (1 g Cr/L) of atomic absorption spectrometry grade (Kanto Chemical Co., Inc., Tokyo, Japan). Deionized water was used throughout the experiments.

1.2.4 Procedures

1.2.4.1 Decomposition procedure of R-1 and SGT11 samples

Glass samples were dried in an oven for 2 h at 110 °C after they were ground with a mortar and pestle. Each ground sample (0.1 g to 0.3 g in weight) was accurately weighed in a PTFE dish and moistened with 1 mL of water. Some samples contained reduced sulfur, and 1 mL of 30 mass% hydrogen peroxide was added to the dish to oxidize the reduced sulfur. To decompose the glass samples, 5 mL of $HClO_4$ and 10 mL of HF were also added to the dish. The dish was placed on a hot plate and heated until perchloric acid fumes were observed. After the dish had cooled, 5 mL of HF was added

19

to the dish. The dish was heated again until perchloric acid fumes were observed. Silicon, which is the main element in glass, was volatilized as silicon fluoride during decomposition. After the dish had cooled, the decomposed solution in the dish was transferred to a 50 mL beaker. The solution was thereafter diluted to approximately 25 mL using 1.8 mol/L $HClO_4$ to form a decomposed sample solution. This decomposed sample solution contained sulfur and other matrix elements that were in the glass.

1.2.4.2 Decomposition procedure of SGT10 samples

Decomposition procedure of SGT10 samples was similar to that of R-1 / SGT11 samples except for the use of an oxidizing agent. Instead of hydrogen peroxide, potassium permanganate (2.5 mL of 0.1 mol/L) was added to the dish to facilitate the strong oxidization of reduced sulfur present in SGT10 samples, which were made of amber glass. Without strong oxidization, reduced sulfur is converted into hydrogen sulfide and evaporated during the decomposition of the samples. Manganese dioxide precipitated after the decomposition of the samples because of the reduction of potassium permanganate. The precipitated manganese dioxide was dissolved by adding 0.5 mL of 3 mass% hydrogen peroxide, which served as a reducing agent here. Fig. 1-1 demonstrates the decomposition procedure of samples.
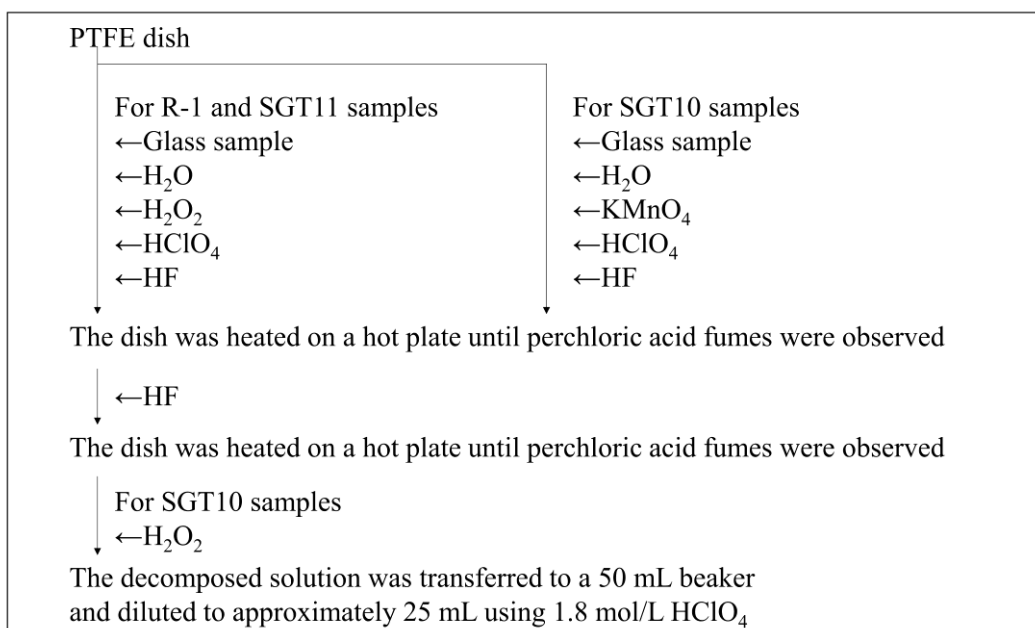
```
┌─────────────────────────────────────────────────────────────────────────────┐
│  PTFE dish                                                                     │
│     │                                                                          │
│     ┌──────────────────────────────────────┐                                  │
│        For R-1 and SGT11 samples          For SGT10 samples                   │
│        ←Glass sample                      ←Glass sample                       │
│        ←H₂O                               ←H₂O                                │
│        ←H₂O₂                              ←KMnO₄                              │
│        ←HClO₄                             ←HClO₄                             │
│        ←HF                                ←HF                                  │
│     │                                      │                                   │
│     ▼                                      ▼                                   │
│  The dish was heated on a hot plate until perchloric acid fumes were observed │
│     │                                                                          │
│     │ ←HF                                                                      │
│     ▼                                                                          │
│  The dish was heated on a hot plate until perchloric acid fumes were observed │
│     │                                                                          │
│     │  For SGT10 samples                                                       │
│     │ ←H₂O₂                                                                   │
│     ▼                                                                          │
│  The decomposed solution was transferred to a 50 mL beaker                     │
│  and diluted to approximately 25 mL using 1.8 mol/L HClO₄                     │
└─────────────────────────────────────────────────────────────────────────────┘
```

Fig. 1-1 Decomposition procedure of samples

1.2.4.3 Separation procedure of sulfur in the samples using an alumina column

For washing, 20 mL of 0.7 mol/L NH_4OH and 10 mL of water were passed through an alumina

column at a flow rate of 20 mL/min using a vacuum kit. For conditioning, 10 mL of 1.8 mol/L $HClO_4$

was passed through the column. The decomposed sample solution was passed through the column at

a flow rate of 2 mL/min to enable the column to absorb the sulfur in the solution. To remove the glass

matrix elements in the solution, 20 mL of 1.8 mol/L $HClO_4$ and 20 mL of water were passed through

the column at a flow rate of 20 mL/min. To desorb sulfur from the column, 10 mL of 0.7 mol/L NH_4OH

was passed through the column at a flow rate of 2 mL/min. The eluent was collected in a 50 mL

volumetric flask and diluted with 0.7 mol/L NH_4OH until its volume was 50 mL. The obtained solution

was named "measurement sample solution". The quantity of sulfur in the solution was determined as

explained in section 1.2.4.5.

1.2.4.4 Recovery of the sulfur in the standard solution

The recovery of sulfur was made using the procedure explained in section 1.2.4.3. A standard solution of sulfur diluted with perchloric acid was introduced in place of the decomposed sample solution (section 1.2.4.3). The standard solutions used were 0.1 to 4.5 mol/L perchloric acid containing 100 μg of sulfur, and 1.8 mol/L perchloric acid containing 5 to 1000 μg of sulfur. After completing the procedure explained in section 1.2.4.3, the sulfur quantity in the measurement sample solution was determined as explained in section 1.2.4.5. The recovery of sulfur is defined as the ratio of the quantity of sulfur determined to the quantity of sulfur introduced. The repeatability of the sulfur recovery was checked using 1.8 mol/L perchloric acid containing 100 μg of sulfur. The experiment was repeated six times using different alumina columns. It was repeated 10 times using the same alumina column to determine whether a column could be used several times.

1.2.4.5 Determination of the sulfur and glass matrix element quantities present in the measurement sample solution

The quantities of sulfur and glass matrix elements present in the measurement sample solution were determined using ICP-AES. The quantities of glass matrix elements were determined using a 0.3 g SGT11 sample. The removal ratio of each glass matrix element was calculated by subtracting the ratio of the quantity of each element determined to its theoretical quantity. The theoretical quantities of glass matrix elements in the 0.3 g SGT11 sample were calculated using the certified composition listed in Table 1-1. Table 2 lists the instrumental conditions of ICP-AES. The sulfur quantity in a glass sample was calculated as sulfur trioxide following the conventions for describing the composition of oxide glass.

Table 1-2 ICP-AES measurement conditions

RF power	1.2 kW
Plasma gas flow	15.0 L/min
Auxiliary gas flow	1.5 L/min
Nebulizer gas pressure	0.75 MPa
Emission line	S(I): 180.669 nm
	Al(I): 167.019 nm
	Na(I): 589.592 nm
	K(I): 766.491 nm
	Mg(II): 279.553 nm
	Ca(II): 396.847 nm
	Fe(II): 259.94 nm
	Ti(II): 334.941 nm
	Cr(II): 205.56 nm

1.2.4.6 Blank test procedure

A blank test was conducted throughout the entire procedure consisting of the decomposition procedure, separation procedure, and determination procedure explained in sections 1.2.4.1, 1.2.4.3, and 1.2.4.5, respectively. The test was repeated 16 times to calculate the mean blank value, standard deviation, detection limit, and quantification limit of sulfur in the samples. The lower limit of detection is defined as the mean of the blank plus three standard deviations. The lower limit of quantification is defined as the mean of the blank plus 10 standard deviations.

1.3 Results and discussions

1.3.1 Study of the separation procedure using an alumina column

Fig. 1-2 displays the recovery of sulfur using various perchloric acid concentrations. The recovery was almost 100% for 0.1 to 4.5 mol/L of perchloric acid. A wide range of perchloric acid concentrations displayed a good recovery. We chose 1.8 mol/L of perchloric acid to dilute the decomposed solution. Fig. 1-3 displays the recovery of sulfur from 5 to 1000 μg. The recovery was between 95 and 102 %. Sulfur in the range of 5 to 30 μg showed a relatively variable recovery. The reason for this variable recovery can be attributed to procedural or measurement errors caused by the small quantity of sulfur present in the samples. The average recovery, which was repeated six times using different alumina columns, was 99.1 %. The standard deviation was 0.25 %. The sulfur quantity in the glass samples has to be between 100 and 1000 μg for the sulfur recovery to exceed 98 %. The average recovery, which was repeated ten times using the same alumina column, was 98.4 % and the standard deviation was 0.33 %. Thus, an alumina column can be used more than once.
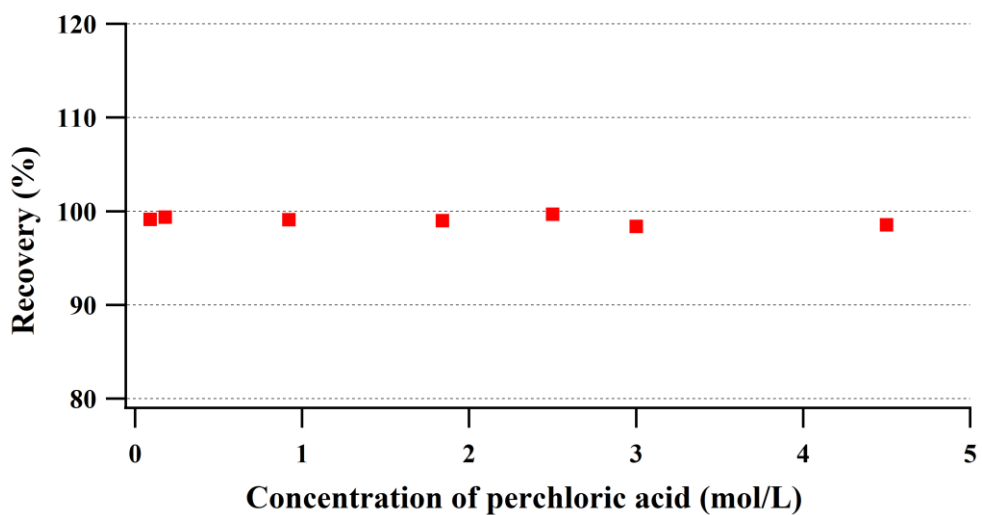
Fig. 1-2 Recovery of 100 μg of sulfur using various perchloric acid concentrations and a separation procedure using an alumina column
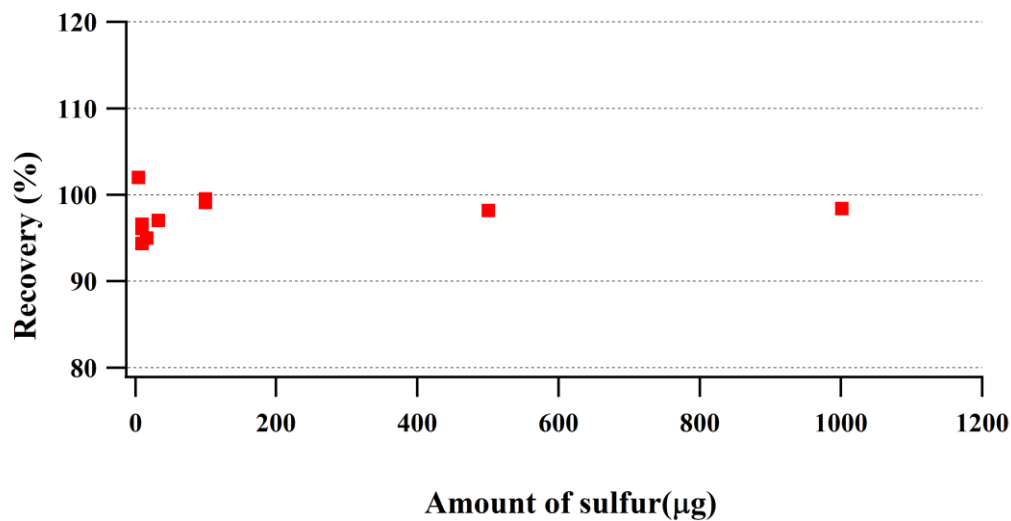

Fig. 1-3 Recovery of 5 to 1000 μg of sulfur with 1.8 mol/L perchloric acid and a separation procedure using an alumina column

1.3.2   Removal of glass matrix elements using an alumina column

Table 1-3 Quantities of glass matrix elements present in the measurement solution, using a 0.3 g of SGT11 sample shows the removal ratios of glass matrix elements when a 0.3 g SGT10 sample was used. The removal ratios were over 99.9 %, except for aluminum. Aluminum has to be an eluent from the alumina column because it was detected even in the blank test. Glass matrix elements were removed by the separation procedure using the alumina column and sulfur was successfully separated from the glass matrix elements.

Table 1-3 Quantities of glass matrix elements present in the measurement solution, using a 0.3 g of SGT11 sample

	Matrix element quantity in the glass sample (μg)	Determined value (μg)	Removal ratio (%)
Al	2900	150	95
Na	30000	<0.1	>99.9
K	1700	<0.1	>99.9
Mg	3900	<0.1	>99.9
Ca	22000	<0.1	>99.9
Fe	720	<0.1	>99.9
Ti	120	<0.1	>99.9
Cr	420	<0.1	>99.9

1.3.3   Determination of the sulfur quantities in R-1 and SGT11 samples

The sulfur quantities in R-1 and SGT11 samples were determined using the procedures explained in sections 1.2.4.1, 1.2.4.3 and 1.2.4.5. Table 1-4 lists the sulfur quantities determined in the form of

oxides. The quantities determined were within the certified values. The relative standard deviations were all within 2 %. The developed procedures shown in sections 1.2.4.1, 1.2.4.3 and 1.2.4.5 were validated to determine the sulfur quantities in R-1 and SGT11 samples accurately.

It took 4–5 h to complete the entire procedure; 2–3 h to decompose a glass sample, 1 h to separate sulfur in a decomposed sample solution using an alumina column, and 1 h to determine the quantity of sulfur in the measurement sample solution using ICP-AES. The procedure can use up to 10 samples simultaneously. The separation procedure using an alumina column is simple. Even any newcomer can easily learn and use the procedure.

Table 1-4 SO$_3$ quantities in R-1 and SGT11 samples

Samples	SO$_3$ (mass%)	
	R-1 (Clear)	SGT11 (Green)
Certified value	**0.20** (0.193-0.204)	**0.06** (0.055-0.069)
N=1	0.198	0.061
N=2	0.195	0.061
N=3	0.202	0.059
Avg.	**0.198**	**0.060**
standard deviation	0.004	0.001
Relative standard deviation (%)	1.8	1.8

1.3.4 Determination of the sulfur quantity in SGT10 sample

Amber soda lime silicate glass contains reduced sulfur, which during decomposition of a sample is converted into hydrogen sulfide and evaporated. Hydrogen peroxide and potassium permanganate were compared to determine the oxidizing agent to be used. A procedure was also implemented without an oxidizing agent. Table 1-5 lists the results of determined quantities of sulfur in SGT10 samples as oxides. With no oxidizing agent, the sulfur quantity was below the lower quantification limit. With 1 mL of 30 mass% hydrogen peroxide, the determined sulfur quantity was lower than the certified value. With 2.5 mL of 0.1 mol/L potassium permanganate, the determined sulfur quantity was within the certified value.

Without oxidizing agents, most of the sulfur in the samples is evaporated as H_2S because reduced sulfur is present in glass in the form of sulfide, as mentioned in XANES studies[11,12]. Hydrogen peroxide was not sufficient to oxidize the sulfide in SGT10 sample during their decomposition. Hydrogen peroxide allowed the evaporation of some of the reduced sulfur as H_2S. Potassium permanganate properly oxidized the sulfide in the SGT10 sample during decomposition and succeeded in preventing the sulfur from evaporating. The process took almost the same time as indicated in section 1.2.4.1. Precipitated manganese dioxide requires approximately 10 min to dissolve. Unlike the method that uses Br_2 as an oxidizing agent, the method using potassium permanganate as the oxidizing agent does not require any additional apparatus or a decomposition procedure.

Table 1-5 Quantities of SO₃ present in SGT10 (amber) samples with and without the oxidizing agents

Oxidizing agent	SO$_3$ (mass%)		
	Without an oxidizing agent	30 % H$_2$O$_2$ 1 mL	0.1 mol/L KMnO$_4$ 2.5 mL
Certified value	**0.05** **(0.043-0.058)**		
N=1	<0.002	0.037	0.053
N=2	<0.002	0.039	0.054
Avg.	<0.002	0.038	0.053

1.3.5   Results of the blank test

The mean blank value of sulfur was 0.49 μg. The standard deviation was 0.25 μg. The limits of detection and quantification were 1.3 and 3.0 μg, respectively. The limit of quantification is low enough to determine the sulfur quantity in soda lime silicate glass because soda lime silicate glass contains over 100 μg/g of sulfur.

The mean blank value of sulfur, 0.49 μg, obtained in this study is much lower than the value obtained in a previous study that used a large alumina column and the large amount of reagents[25]. The higher blank value obtained in this previous study would have been due to the small quantities of sulfur contained in the large alumina column and the reagents. In our study, we reduced the blank value of sulfur with a decomposition procedure that used hydrofluoric acid and perchloric acid, and a separation procedure that used a small and high-purity alumina column. However, the mean blank value of sulfur obtained in the study, 0.49 μg, is 10 times higher than the value obtained in the study done by

Makishima[22], who purified the reagents for decomposition and used two charcoal filters in a flow injection system to reduce sulfur contamination. These processes are not required in our method because our limit of quantification of sulfur is low enough to determine the quantity of sulfur in soda lime silicate glass as mentioned above.

1.4　Conclusions

A simple, rapid, and accurate method to determine the sulfur quantity in soda lime silicate glass was investigated. Glass samples were decomposed using hydrofluoric acid, perchloric acid, and an oxidizing agent. Potassium permanganate was used as the oxidizing agent with glass samples containing reduced sulfur, such as those made of amber glass. The decomposed solution was diluted using perchloric acid. The sulfur in the decomposed solution was adsorbed on the alumina column and was separated from the glass matrix elements by rinsing with diluted perchloric acid. The sulfur was desorbed from the column by passing diluted ammonia through the column. ICP-AES was used to determine the sulfur quantity in the ammonia eluent. The method requires approximately 0.1 to 0.3 g glass samples depending on the sulfur quantity in the glass. The separation procedure with the alumina column is simple and rapid: it takes only 1 h, and it can simultaneously treat up to 10 samples. The method was validated using three certified glass samples. The sulfur values determined are within the certified values. The relative standard deviations of the sulfur values were less than 2 %. This method does not require any special apparatus to decompose a glass sample.

1.5 References

[1]   Green Rhino Energy: Value Chain Activity: Manufacturing Solar Glass, http://www.greenrhinoenergy. com/solar/industry/ind_15_solarglass.php (accessed May 11, 2022).

[2]   L.A.B. Pilkington, The float glass process, Proceedings of the Royal Society of London. Series A, Mathematical and Physical Sciences. 314 (1969) 1–25. https://doi.org/10.1098/rspa.1969.0212.

[3]   D.W. Readey, A.R. Carper Jr, Molecular diffusion with a moving boundary and spherical symmetry, Chemical Engineering Science. 21 (1966) 917–922. https://doi.org/10.1016/0009-2509(66)85085-6.

[4]   M. CABLE, Kinetics and Mechanisms of Fining Glasses, Journal of the American Ceramic Society. 49 (1966). https://doi.org/10.1111/j.1151-2916.1966.tb15412.x.

[5]   J. Kloužek, M. Arkosiová, L. Němec, P. Cincibusová, The role of sulphur compounds in glass melting, Glass Technology: European Journal of Glass Science and Technology Part A. 48 (2007) 176–182.

[6]   M. Hujová, M. Vernerová, Influence of fining agents on glass melting: A review, part 1, Ceramics - Silikaty. 61 (2017) 119–126. https://doi.org/10.13168/cs.2017.0006.

[7]   R.G.C. Beerkens, Amber chromophore formation in sulphur- and iron-containing soda-lime-silica glasses, Glass Science and Technology. 76 (2003) 166–175.

[8]   R.G.C. Beerkens, Sulphate decomposition and sulphur chemistry in glass melting processes, Glass Technology. 46 (2005) 39–46.

[9]   R.G.C. Beerkens, Sulfate Decomposition and Sodium Oxide Activity in Soda-Lime-Silica Glass Melts, Journal of the American Ceramic Society. 86 (2003) 1893–1899. https://doi.org/10.1111/j.1151-2916.2003.tb03578.x.

[10] R.G.C. Beerkens, K. Kahl, Chemistry of sulphur in soda-lime-silica glass melts, Physics and Chemistry of Glasses. 43 (2002) 189–198.

[11] E. Paris, G. Giuli, M.R. Carroll, I. Davoli, The valence and speciation of sulfur in glasses by x-ray absorption spectroscopy, Canadian Mineralogist. 39 (2001) 331–339. https://doi.org/10.2113/gscanmin.39.2.331.

[12] L. Backnaes, J. Stelling, H. Behrens, J. Goettlicher, S. Mangold, O. Verheijen, R.G.C. Beerkens, J. Deubener, Dissolution mechanisms of tetravalent sulphur in silicate melts: Evidences from sulphur K edge XANES studies on glasses, Journal of the American Ceramic Society. 91 (2008) 721–727. https://doi.org/10.1111/j.1551-2916.2007.02044.

[13] F.L. Harding, Effect of base glass composition on amber colour, Glass Technology. 13 (1972) 43–49.   https://pascal-francis.inist.fr/vibad/index.php?action=getRecordDetail&idt=PASCAL7388000957 (accessed November 26, 2021).

[14] P.A. Webster, A.K. Lyle, Short Methods for Chemical Analysis of Glass, Journal of the American Ceramic Society. 23 (1940) 235–241. https://doi.org/10.1111/j.1151-2916.1940.tb14262.x.

[15] L. Gustafsson, Determination of ultramicro amounts of sulphate as methylene blue-I. The colour reaction, Talanta. 4 (1960) 227–235.

[16] O.H. Kriege, A.L. Wolfe, The spectrophotometric determination of sulphur in iron alloys. Methylene blue method, Talanta. 9 (1962) 673–678.

[17] Y. Arikawa, T. Ozawa, I. Iwasaki, Determination of total-sulfur in igneous rocks with tin(II)-strong phosphoric acid, BUNSEKI KAGAKU. 21 (1972) 920–924. https://doi.org/10.2116/bunsekikagaku.21.920.

[18] T. Yarita, A. Masui, M. Noshiro, Analysis of total- and sulfide- sulfur in silicate glasses by

using strong phosphoric acid in combination with ion chromatography, Research Report of Asahi Glass Co., Ltd. 37 (1987) 37–42.

[19]   J.M. Murphy, G.A. Sergeant, A Method for the Determination of Total Sulphur in Silicate Rocks, Analyst. 99 (1974) 515–518.

[20]   E. Toda, Y. Kubota, G. Ichikawa, Determination of trace sulfur by ICP-AES with gas-phase sample introduction technique., BUNSEKI KAGAKU. 41 (1992). https://doi.org/10.2116/bunsekikagaku.41.9_453.

[21]   M. Kawamoto, M. Kagaya, R. Akiyama, Selective determination of trace amounts of total and sulfate-sulfur in glasses, Research Report of Asahi Glass Co., Ltd. 48 (1998) 11–19.

[22]   A. Makishima, E. Nakamura, Determination of total sulfur at microgram per gram levels in geological materials by oxidation of sulfur into sulfate with in situ generation of bromine using isotope dilution high-resolution ICPMS, Analytical Chemistry. 73 (2001) 2547–2553. https://doi.org/10.1021/ac001550i.

[23]   E. Guadagnino, P. Sundberg, D. Brochot, A collaborative study into the determination of boron in glass using x-ray fluorescence (XRF) spectroscopy, Glass Technology: European Journal of Glass Science and Technology Part A. 47 (2006) 103–111.

[24]   Standard Test Methods for Chemical Analysis of Soda-Lime and Borosilicate Glass, ASTM C169-16, ASTM International, 2016.

[25]   F. Nydahl, Determination of Sulfur in Iron and Steel by Barium Chloride Method, Analytical Chemistry. 26 (1954) 580–584. https://doi.org/10.1021/ac60087a054.

Chapter2

Separation and Determination of Sulfide Sulfur and Sulfate Sulfur in Soda Lime Silicate Glass

2.1   Introduction

Quantitative determination of sulfide sulfur and sulfate sulfur and the average valence of sulfur in soda lime silicate glass are important because they affect the number of bubble defects and glass color. Sodium sulfate (Na_2SO_4) is commonly added as a source of sulfur in the production of soda lime silicate glass. It works as a fining agent and coloring agent. It reduces the number of bubbles in the glass as a fining agent. The melting and fining reactions were investigated. The fining mechanism is due to oxidation-reduction reactions of sulfur to produce SO_2 and O_2 gases. Sodium sulfate gives an amber color to glass as a coloring agent with iron and reducing agents. Sulfate reacts with reducing agents to produce sulfide. Ferric iron – sulfide – alkali chromospheres are said to create the amber color[1,2]. As described, sulfur remains in glass after oxidation-reduction reactions in the form of sulfide sulfur and sulfate sulfur[3,4].

A method that determines sulfide and sulfate in glass is required. It is expected that the quantities of sulfide and sulfate can be determined accurately and precisely by separating them. Furthermore, a method with commonly used equipment is preferable because it can be implemented in laboratories in glass production sites. We describe our proposed method after reviewing the determination methods of the total quantity of sulfur in glass and the determination methods of sulfide and sulfate quantities, and/or the valence state of sulfur in glass.

Many methods are already available to determine the total quantity of sulfur in a glass material. Chemical analysis methods include gravimetric analysis of barium sulfate[5], combustion separation – hydrogen peroxide trap and sodium borate titration[6], tin(II)-strong phosphoric acid decomposition

- iodometric titration[7], tin(II)-strong phosphoric acid decomposition – ion chromatography[8], hydrophosphorous acid – hydroiodic acid reduction[9], sodium iodide – hydroiodic acid – hypophosphorous acid reduction[10], isotope dilution high-resolution inductively coupled plasma mass spectrometry equipped with a flow injection system[11], and hydrofluoric acid – oxidizing agent decomposition – alumina column separation[12]. X-ray fluorescence analysis (XRF)[13,14] and infrared detection of SO_2 formed after high-temperature combustion[15,16] are examples of direct analysis without chemical treatment.

Several methods are also available to determine sulfide and sulfate and/or the valence state of sulfur in glass or other materials. Nagashima et al. reported a determination method of total sulfur and sulfide in igneous rocks with tin(II)-strong phosphoric acid and strong phosphoric acid, respectively[17]. Yarita et al. applied the method to glass [8]. The method determines the small quantity of total sulfur and sulfide (10 μg/g) using a small number of glass samples (approximately 0.1 g). However, this method has some drawbacks. One is that it determines total sulfur and sulfide with two experiments. The quantity of sulfate was calculated from the total sulfur and sulfide determined. The other drawback is that reduction reagents (tin(II)-strong phosphoric acid and strong phosphoric acid) must be synthesized beforehand. Sieger tried hydrofluoric acid decomposition under an inert atmosphere combined with a hydrogen sulfide trap with $AgNO_3$ titration to determine sulfide in a bottom surface layer of a float glass[18]. However, the study did not show the details of the procedure enough for reproducible determination. Guadagnino et al. used a hydrogen sulfide trap with silver nitrate and determined the excess silver by flame atomic absorption spectrometry to determine the quantity of sulfide in glass[19]. However, the method did not determine the quantity of total sulfur or sulfate. Sato et al. used wavelength-dispersive X-ray fluorescence spectrometric analysis (WD-XRF) and obtained the peak shift of S-Kα with various sulfur-containing materials [20]. This method eliminates chemical pretreatments and is a nondestructive analysis. However, its energy resolution is insufficient to resolve

36

S-Kα due to the single-crystal system; the average valence of sulfur is solely obtained from the S-Kα peak shift. Faessler et al.[21] and Goshi et al.[22] used high-resolution wavelength-dispersive X-ray fluorescence spectrometric analysis with two crystals to precisely measure S-Kα. The method measured some sulfur-containing reference materials, and it deconvoluted the S-Kα spectra to calculate the ratio of each valence of sulfur. However, it has some drawbacks. It has a low signal-to-noise ratio due to the two-crystal system. The analysis time is long to obtain a good signal-to-noise ratio enough for glass materials because the quantity of sulfur in glass materials is small. This method requires reference materials or a different method to determine the quantity of total sulfur. Furthermore, the equipment is not widely used. Paris et al.[3], Fleet[23], and Backnaes et al.[4] applied X-ray absorption near-edge (XANES) to rock and glass materials. The method estimated the valence state of sulfur in glass materials by comparing the peak position with some sulfur-containing reference materials. These studies[3,4] showed that glass samples contained sulfide and sulfate but did not contain sulfite. A drawback of this method is that the peak positions of sulfide reference materials are not constant. It is impossible to generate a calibration curve between the sulfur valence of reference materials and their peak positions. Alonso-Mori et al. also confirmed this drawback and showed that S-Kα energy shifts measured by X-ray emission spectroscopy (XES) using a synchrotron radiation facility can be used for a quantitative determination of the ratio of different sulfur species[24]. The XANES and XES methods have a similar drawback in that they require the use of synchrotron radiation facilities. A wavelength analysis of X-ray emission spectra using the electron microprobe was studied to measure the valence state of sulfur, but the beam damage is a problem [25]. Raman spectroscopy identified sulfide and sulfate in silicate glass, but the quantitative determination is a challenge [26].

As mentioned above, there is no method that determines sulfide and sulfate with commonly used equipment. The purpose of this study is to develop a new method that determines sulfide and sulfate

in soda lime silicate glass with commonly used equipment and confirm the accuracy and precision. In this study, we follow and improve hydrogen sulfide trap methods [18,19]. We propose a determination method that consists of the decomposition of a glass sample and separation and determination of sulfide and sulfate. For our proposed method, a ground glass sample is decomposed with hydrofluoric acid and hydrochloric acid in a decomposition vessel combined with a series of traps. Hydrofluoric acid dissolves silicon dioxide networks in glass. Hydrochloric acid dissolves the glass matrix elements. Sulfide in the sample volatilizes as hydrogen sulfide during decomposition because the decomposition solution is strongly acidic. A nitrogen stream is added to prevent the oxidation of sulfide during decomposition and to carry volatilized hydrogen sulfide to the series of traps that contain sodium hydroxide and hydrogen peroxide solution. The solution absorbs hydrogen sulfide. Volatilized and trapped sulfide is measured by inductively coupled plasma atomic emission spectroscopy (ICP-AES). Sulfate remains in the decomposition vessel after decomposition. Sulfate is measured by ICP-AES after a volatilization process of hydrofluoric acid and hydrochloric acid via heating and a separation process using an alumina column [12]. The method can determine sulfide and sulfate with commonly used equipment in laboratories. The total sulfur is calculated as the sum of sulfide and sulfate. The developed method is applied to two glass reference materials. The determined total sulfur quantities in the reference materials are compared with certified sulfur values. The average valences of sulfur, calculated from the quantities of sulfide and sulfate determined, are compared with the average valences of sulfur measured by WD-XRF. As glass materials contain sulfide and sulfate[3,4], we validate the new method by showing that the sums of sulfide and sulfate match the certified values and that the average valences match the results of WD-XRF.

2.2　Experimental

2.2.1　Glass materials

Two standard reference soda lime silicate glass materials were used in the experiment: SRM 1831 (National Institute of Standards and Technology, Gaithersburg, The United States of America) and SGT10 (Society of Glass Technology, Sheffield, United Kingdom). SRM 1831 and SGT10 represent clear and amber glass, respectively. Table 2-1 lists the certified mass fractions of the two glass reference materials. Values in parentheses indicate 95 % confidence intervals. All elements are listed in the form of oxides with the maximum valence of each element, regardless of the real valence, following the conventions for describing the composition of oxide glass. For example, iron (Fe) is contained in glass materials as ferrous (Fe^{2+}) and ferric (Fe^{3+}) but listed as Fe_2O_3. Sulfur (S) is contained in glass materials as sulfide (S^{2-}) and sulfate (S^{6+}) but listed as SO_3.

The glass samples were dried in an oven for 2 h at 110 °C after they were ground with a mortar and pestle and used for the determination of sulfide and sulfate. For valence analysis by WD-XRF, the surfaces of glass samples were mirror-polished using cerium oxide. Three polished glass samples of each of the two types of glass were prepared.

Table 2-1 Certified mass fractions of glass reference materials

Certified mass fractions (mass%)

	SRM 1831 (Clear)	SGT10 (Amber)
SiO_2	73.08 (73.00-73.16)	72.7 (72.64-72.72)
Al_2O_3	1.21 (1.17-1.25)	1.62 (1.587-1.644)
Na_2O	13.32 (13.27-13.37)	12.2 (12.17-12.23)
K_2O	0.33 (0.31-0.35)	0.35 (0.344-0.357)
MgO	3.51 (3.46-3.56)	1.81 (1.807-1.820)
CaO	8.20 (8.15-8.25)	10.7 (10.61-10.75)
BaO	-	0.02 (0.020-0.022)
Fe_2O_3	0.087 (0.084-0.090)	0.33 (0.317-0.322)
TiO_2	0.019 (0.017-0.021)	0.097 (0.095-0.099)
Cr_2O_3	-	0.02 (0.018-0.022)
SO_3	0.25 (0.240-0.260)	0.05 (0.043-0.058)

2.2.2   Inorganic reference materials

Four inorganic reference materials that contain a specific valence of sulfur were used as the standard materials for the WD-XRF measurement: S^{6+}, strontium sulfate (FUJIFILM Wako Pure Chemical Corporation, Osaka, Japan); S^{4+}, potassium disulfite of special grade (Kanto Chemical Co., Inc., Tokyo, Japan); S^{2+}, sodium thiosulfate pentahydrate of special grade (Kanto Chemical Co., Inc., Tokyo, Japan); and S^{2-}, zinc sulfide of high purity grade (Sigma-Aldrich Japan, Tokyo, Japan). These reference materials were ground with a mortar and pestle and pressed to make pellets using aluminum rings.

2.2.3   Apparatus and instrumentation

A polytetrafluoroethylene (PTFE) decomposition vessel was used to decompose the glass samples with reagents. A magnetic stirrer and a 40×7 mm^2 stirring bar were used to stir the samples and reagents in the vessel. A 100 mL polypropylene separatory funnel with a stopcock was used to add reagents to the vessel. Three 30 mL polypropylene cups were used as trap containers. A 100 mL PTFE dish was used to volatilize hydrofluoric acid and hydrochloric acid as well as silicon oxide matrix in the glass decomposed solution. A 100 mL and a 50 mL volumetric flask were used. An alumina column, InterSep AL-N Al$_2$O$_3$ 500 mg/2 mL (GL Sciences Inc., Tokyo, Japan), placed on a vacuum filtration kit (GL Sciences Inc., Tokyo, Japan) was used to separate the sulfur from glass matrix elements[12]. An inductively coupled plasma atomic emission spectrometer (SPS5520, Hitachi High-Tech Corporation, Tokyo, Japan) was used to determine the sulfur quantity. A wavelength-dispersive X-ray fluorescence spectrometer (ZSX100e, Rigaku Corporation, Tokyo, Japan) was used to measure S-Kα spectra.

2.2.4   Reagents and chemicals

Hydrofluoric acid (50 mass%), hydrochloric acid (36 mass%), perchloric acid (60 mass%), ammonia solution (25 mass%) of atomic absorption spectrometry grade (Kanto Chemical Co., Inc., Tokyo, Japan), hydrogen peroxide (30 mass%) and sodium hydroxide of special grade (Kanto Chemical Co., Inc., Tokyo, Japan) were used. The standard solution used for the ICP-AES analysis was sulfate ion standard solution (1 g SO$_4^{2-}$/L) of ion chromatography grade (Kanto Chemical Co., Inc., Tokyo, Japan). Deionized water was degassed and used throughout the experiments.

2.2.5   Procedures

2.2.5.1   Decomposition of glass materials and the separation of sulfide and sulfate

Fig. 2-1 demonstrates the apparatus for the decomposition of glass samples to separate sulfide and sulfate. A 0.5 g aliquot of the ground glass sample was accurately weighed in a PTFE decomposition vessel and moistened with 1 mL of water. A mixture of 4 mL of 12 mol/L HF and 10 mL of 6 mol/L HCl was added to the polypropylene separatory funnel on the vessel. A mixture of 10 mL of 0.3 mol/L hydrogen peroxide and 0.025 mol/L sodium hydroxide was added to each of the three 30 mL polypropylene cups.

To expel oxygen in the decomposition vessel, nitrogen gas was passed through at approximately 10 mL per second for 5 minutes. A mixture of HF and HCl solution in the funnel was added to the decomposition vessel by twisting the stopcock and the three-way cock. Glass samples were decomposed with stirring for 90 minutes with nitrogen flow at approximately 10 mL per second.

After decomposition, the solution in the trap cups was transferred to a 50 mL volumetric flask. A small amount of water was added to each of the cups and each of the flow channels to wash them, the water was transferred to the same 50 mL volumetric flask, and the solution was diluted to the mark of the flask with water.

The decomposition vessel was opened, and 1 mL of 1 mol/L hydrogen peroxide was added to oxidize any sulfur components in the decomposed solution to sulfate. The solution in the vessel was transferred to a PTFE dish. A small amount of water was added to the vessel to wash it and transferred to the dish. After 5 mL of $HClO_4$ was added to the dish, the dish was placed on a hot plate. It was heated until perchloric acid fumes were observed to volatilize hydrofluoric acid, hydrochloric acid, and silicon as silicon fluoride. After the dish had cooled, the decomposed solution in the dish was transferred to a 50 mL beaker. The solution was thereafter diluted to approximately 25 mL using 1.8

mol/L HClO$_4$. Sulfur in the form of sulfate in the solution was separated using an alumina column [12].
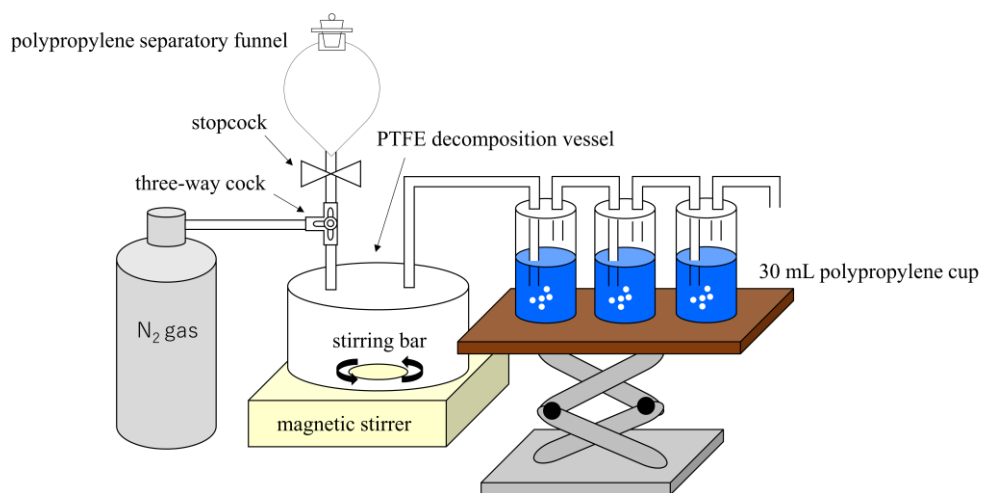

Fig. 2-1 Components of the apparatus for decomposition and a trap. Glass materials are decomposed in the PTFE decomposition vessel with nitrogen flow. Sulfide in glass materials is volatilized as hydrogen sulfide and trapped by a mixture of hydrogen peroxide and sodium hydroxide in polypropylene cups.

2.2.5.2   Sulfur determination and calculation of the average sulfur valence

The quantities of sulfur present in the solution after separation with the alumina column and the solution collected from the trap cups were determined by ICP-AES. Table 2-2 lists the instrumental conditions of ICP-AES. The sulfide quantity and sulfate quantity in the glass material were calculated as sulfur trioxide following the conventions for describing the composition of oxide glass. The total sulfur quantity was calculated by adding sulfide quantity and sulfate quantity, written as sulfur trioxide. The average sulfur valences in glass materials were calculated by subtracting eight times the sulfide

quantity divided by the sum of sulfate and sulfide quantities from six as follows:

$$\text{The average sulfur valence} = 6 - 8 \times \frac{S^{2-} \text{ (as } SO_3 \text{ mass\%)}}{S^{2-} \text{ (as } SO_3 \text{ mass\%)} + S^{6+} \text{ (as } SO_3 \text{ mass\%)}} \cdots (2-1)$$

Table 2-2 Instrumental conditions of ICP-AES

RF power	1.2 kW
Plasma gas flow	15.0 L/min
Auxiliary gas flow	1.5 L/min
Nebulizer gas pressure	0.75 MPa
Emission line	S(I): 180.669 nm

2.2.5.3　　Blank test procedure

A blank test was conducted throughout the entire procedure consisting of the decomposition procedure, the separation procedure, and the determination procedure. The test was repeated four times to calculate the mean blank value and standard deviation. The limit of detection is defined as the mean blank value plus threefold standard deviations. The limit of quantification was defined as the mean blank value plus tenfold standard deviations.

2.2.5.4　　S-Kα spectra measurement and determination of the average sulfur valence procedure by WD-XRF

S-Kα spectra were measured by the WD-XRF. The X-ray tube for primary excitation was a rhodium anode X-ray tube with input conditions of 30 kV and 120 mA and operated under vacuum conditions. S-Kα spectra were measured using a NaCl crystal with a fine slit and a gas flow proportional counter

with an argon-methane mixture. Spectra were scanned every 0.020 degrees with 1.5 s per scan from 143.5 to 146.0 degrees (2-theta angle). The abscissa was changed from the 2-theta angle to the energy. The obtained spectra were deconvoluted into two Gaussian curves, which correspond to S-Kα1 and S-Kα2. The peak with a higher energy value (S-Kα1) was used as the peak position. Each pellet was measured four times, and the mean of the peak energy value and the 95 % confidence intervals were calculated.

2.3   Results and discussions

2.3.1   Detection limit and quantification limit

The mean blank value, detection limit, and quantification limit of sulfide trapped were 1.5, 2.5, and 4.9 μg/g in sulfur trioxide form, respectively. The mean blank value, detection limit, and quantification limit of sulfate remaining in the decomposition vessel were 1.7, 2.4, and 3.8 μg/g in sulfur trioxide form, respectively. The limit of quantification of sulfide was lower than those in the studies performed by Nagashima et al. [17]and Yarita et al. [8], which were approximately 10 μg/g. Their limits of quantification of sulfate were not clear because the quantities of sulfate were calculated by subtracting the quantities of sulfide from the quantities of total sulfur. If we compare their lower limits of quantification of total sulfur, which were also approximately 10 μg/g, with our lower limit of quantification for sulfate, ours was lower than theirs.

2.3.2   Determination of sulfide and sulfate in glass reference materials

Table 2-3 lists the quantities of sulfide and sulfate in two glass reference materials in the form of sulfur trioxides. It also lists the average valence of sulfur in two glass reference materials determined by the method shown in sections 2.2.5.1 and 2.2.5.2. The method determined sulfide and sulfate. The quantity of sulfide and sulfate in SRM 1831 was under the detection limit and 0.247 ± 0.009 mass%

(average ± 95 % confidence intervals), respectively. The quantities of sulfide and sulfate in SGT10 were 0.0480 ± 0.0002 and 0.020 ± 0.0002 mass%, respectively. The total sulfur quantities, which are the sum of sulfide and sulfate, were within the range of each of the certified values.

The average valence of sulfur of SRM 1831 calculated from quantities of sulfide and sulfate was 6.00, as sulfide was not detected. The average valence of sulfur in SGT10 calculated from the quantities of sulfide and sulfate was -1.68 ± 0.05.

Table 2-3 Quantities of sulfide, sulfate, and the total sulfur in glass reference materials in the form of sulfur trioxides and the average valences of sulfur determined by the decomposition and trap procedure

		Sulfur value in SO_3 form (mass%)			Average valence
		Sulfide	Sulfate	Total Sulfur	of Sulfur
SRM 1831	Certified Value	-	-	0.25 (0.24-0.26)	-
	N=1	n.d.	0.246	0.246	6.00
	N=2	n.d.	0.246	0.246	6.00
	N=3	n.d.	0.250	0.250	6.00
	Avg.	n.d.	0.247	0.247	6.00
	standard deviation	-	0.0021	0.0021	-
	Relative standard deviation (%)	-	0.85	0.85	-
	95 % confidence intervals	-	0.009	0.009	-
SGT10	Certified Value	-	-	0.05 (0.043-0.058)	-
	N=1	0.0481	0.0019	0.0500	-1.70
	N=2	0.0479	0.0021	0.0500	-1.66
	N=3	0.0479	0.0021	0.0500	-1.66
	N=4	0.0481	0.0018	0.0499	-1.71
	Avg.	0.0480	0.0020	0.0500	-1.68
	standard deviation	0.0002	0.0001	0.0005	0.024
	Relative standard deviation (%)	0.3	5.8	0.1	1.4
	95 % confidence intervals	0.0002	0.0002	0.001	0.05

2.3.3 Valence analysis of sulfur in glass reference materials by WD-XRF

Fig. 2-2 shows normalized S-Kα X-ray emission spectra of four inorganic reference materials containing sulfur in different valences from -2 to 6. By increasing the sulf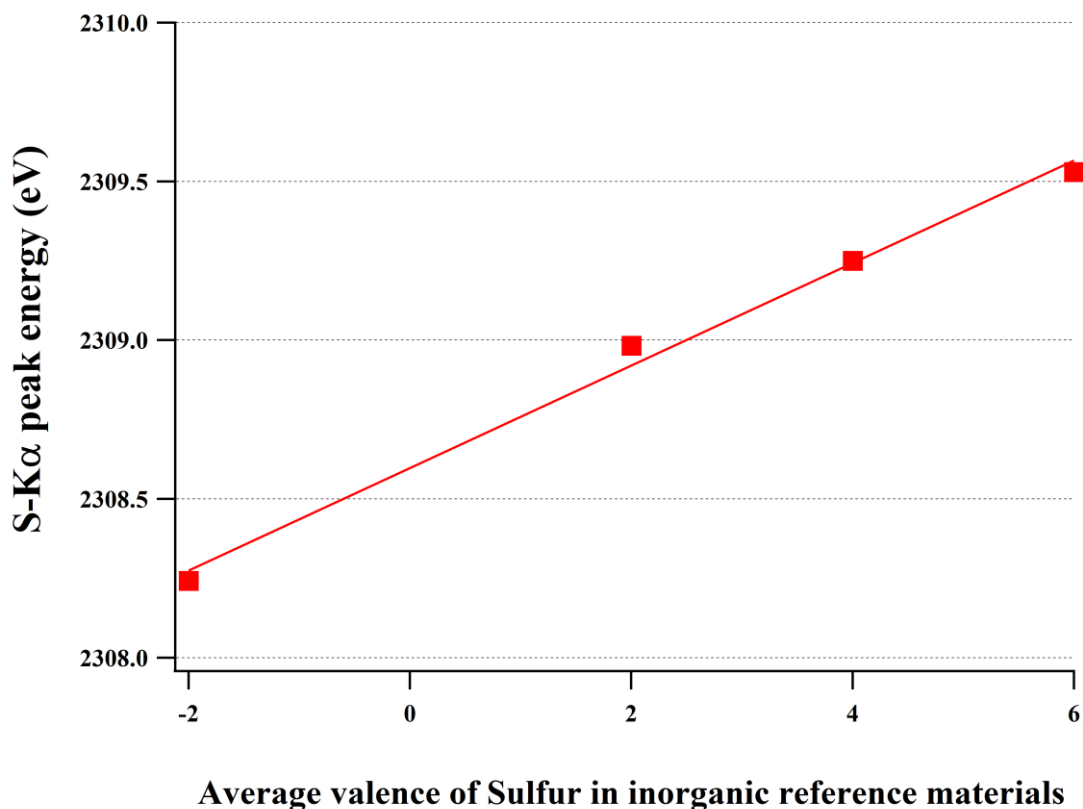ur valence, the peak energy of S-Kα increases. Fig. 2-3 presents a correlation between the specific valences of sulfur in inorganic reference materials and their S-Kα1 peak energies. A calibration curve with good linearity is obtained, and the correlation coefficient is 0.997. The standard errors of peak energies calculated from four measurements were all under 0.02 eV. The size of the points covers the error bars (vertical bars). From the calibration curve, the average sulfur valences of SRM 1831 and SGT10 were 5.9 ± 0.1 and -1.6 ± 0.2 (average ± 95 % confidence intervals), respectively.
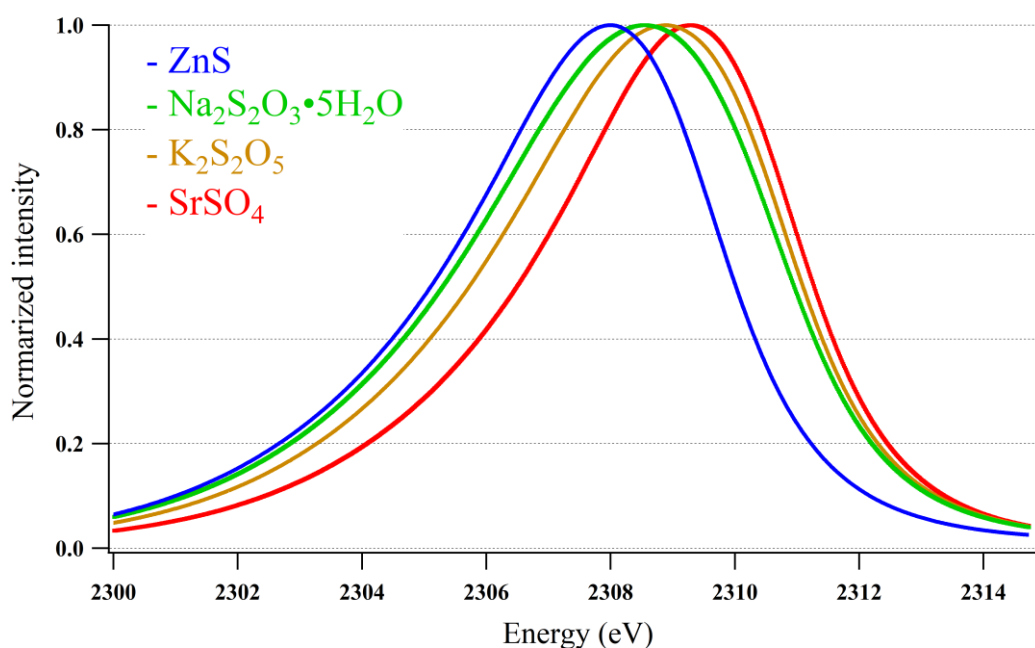
Fig. 2-2 Normalized S-Kα X-ray emission spectra of strontium sulfate, potassium disulfite, sodium thiosulfate pentahydrate, and zinc sulfide

Fig. 2-3 Correlation between the specific valences of sulfur in inorganic reference materials and their S-Kα peak energies and the calibration curve measured by WD-XRF. The size of the points covers the 95 % confidence intervals.

2.3.4   Comparison of the decomposition-separation method with WD-XRF for valence analysis

Table 2-4 shows a comparison of the average sulfur valences of glass reference materials between the proposed decomposition and separation method and the WD-XRF. The average sulfur valences for the two glass reference materials using the proposed method are in good agreement with those measured by WD-XRF.

The proposed method shows that the sums of sulfide and sulfate of two glass reference materials were within the certified values, and the average sulfur valences matched the results of WD-XRF. It

49

was validated to determine sulfide and sulfate in two glass reference materials. It determines sulfide

and sulfate with commonly used equipment in laboratories.

Table 2-4 Comparison of the average sulfur valences of glass reference materials between the proposed decomposition and separation method and the WD-XRF

	The proposed decomposition and separation method	WD-XRF
SRM 1831	6.00	5.9 ± 0.1
SGT10	-1.68 ± 0.05	-1.6 ± 0.2

2.4　　　Conclusions

A new determination method for sulfide and sulfate in soda lime silicate glass is investigated. The method separates and determines sulfide and sulfate. Glass samples are decomposed under nitrogen flow with hydrochloric acid and hydrofluoric acid in a decomposition vessel, which is combined with a series of three traps containing sodium hydroxide and hydrogen peroxide. Sulfide in the form of hydrogen sulfide volatilizes and is absorbed in the trap solution, while sulfate remains in the decomposition solution. Sulfide and sulfate are determined by ICP-AES. The method can be implemented in laboratories in glass production sites because it uses a commonly used apparatus and equipment. The method is tested on two glass reference materials and determines sulfide and sulfate with under 1 % relative standard deviations when the quantities are over 0.05 mass% in sulfur trioxide form. The quantification limits of sulfide and sulfate are under 5 μg/g in sulfur trioxide form. The quantities of total sulfur, which are calculated as the sums of sulfide and sulfate, are within the range of each certified value. The average sulfur valences for the two glass reference materials obtained by the method are in good agreement with those obtained by WD-XRF. The WD-XRF can be used as a routine analysis to measure average sulfur valences in glass materials and our developed method can be used as a validation method or for a standard creation.

2.5   References

[1]   F.L. Harding, Effect of base glass composition on amber colour, Glass Technology. 13 (1972) 43–49.

[2]   R.G.C. Beerkens, Amber chromophore formation in sulphur- and iron-containing soda-lime-silica glasses, Glass Science and Technology. 76 (2003) 166–175.

[3]   E. Paris, G. Giuli, M.R. Carroll, I. Davoli, The valence and speciation of sulfur in glasses by x-ray absorption spectroscopy, Canadian Mineralogist. 39 (2001) 331–339. https://doi.org/10.2113/gscanmin.39.2.331.

[4]   L. Backnaes, J. Stelling, H. Behrens, J. Goettlicher, S. Mangold, O. Verheijen, R.G.C. Beerkens, J. Deubener, Dissolution mechanisms of tetravalent sulphur in silicate melts: Evidences from sulphur K edge XANES studies on glasses, Journal of the American Ceramic Society. 91 (2008) 721–727. https://doi.org/10.1111/j.1551-2916.2007.02044.

[5]   P.A. Webster, A.K. Lyle, Short Methods for Chemical Analysis of Glass, Journal of the American Ceramic Society. 23 (1940) 235–241. https://doi.org/10.1111/j.1151-2916.1940.tb14262.x.

[6]   W. Fletcher, Combustion separation techniques in glass analysis, Glastech Ber. 44 (1971) 462–466.

[7]   Y. Arikawa, T. Ozawa, I. Iwasaki, Determination of total-sulfur in igneous rocks with tin(II)-strong phosphoric acid, BUNSEKI KAGAKU. 21 (1972) 920–924. https://doi.org/10.2116/bunsekikagaku.21.920.

[8]   T. Yarita, A. Masui, M. Noshiro, Analysis of total- and sulfide- sulfur in silicate glasses by using strong phosphoric acid in combination with ion chromatography, Research Report of Asahi Glass Co., Ltd. 37 (1987) 37–42.

[9]   E. Toda, Y. Kubota, G. Ichikawa, Determination of trace sulfur by ICP-AES with gas-phase

sample introduction technique., BUNSEKI KAGAKU. 41 (1992) 453–458. https://doi.org/10.2116/bunsekikagaku.41.9_453.

[10] M. Kawamoto, M. Kagaya, R. Akiyama, Selective determination of trace amounts of total and sulfate-sulfur in glasses, Research Report of Asahi Glass Co., Ltd. 48 (1998) 11–19.

[11] A. Makishima, E. Nakamura, Determination of total sulfur at microgram per gram levels in geological materials by oxidation of sulfur into sulfate with in situ generation of bromine using isotope dilution high-resolution ICPMS, Analytical Chemistry. 73 (2001) 2547–2553. https://doi.org/10.1021/ac001550i.

[12] Y. Saijo, Y. Suzuki, R. Akiyama, K. Miura, Determination of sulfur in soda-lime silicate glass by inductively coupled plasma atomic emission spectroscopy following separation using an alumina column, Journal of the Ceramic Society of Japan. 129 (2021) 54–59. https://doi.org/10.2109/jcersj2.20185.

[13] P.J. Potts, A handbook of silicate rock analysis8, in: Blackie, Glasgow, 1987.

[14] E. Guadagnino, P. Sundberg, D. Brochot, A collaborative study into the determination of boron in glass using x-ray fluorescence (XRF) spectroscopy, Glass Technology: European Journal of Glass Science and Technology Part A. 47 (2006) 103–111.

[15] S. Terashima, The rapid determination of total carbon and sulfur in geological materials by combustion and infrared absorption photometry, Analytica Chimica Acta. 101 (1978) 25–31. https://doi.org/10.1016/S0003-2670(01)83836-8.

[16] S. Terashima, Determination of Total Carbon and Sulfur in Fifty-two Geochemical Reference Samples by Combustion and Infrared Absorption Spectrometry, Geostandards Newsletter. 12 (1988) 249–252. https://doi.org/10.1111/j.1751-908X.1988.tb00052.x.

[17] S. Nagashima, M. Yoshida, T. Ozawa, The Determination of Sulfide- and Sulfate-Sulfur in Igneous Rocks with Tin(II)-Strong Phosphoric Acid and Strong Phosphoric Acid, Bull Chem

Soc Jpn. 45 (1972) 3446–3451. https://doi.org/10.1246/bcsj.45.3446.

[18]   J.S. Sieger, Chemical characteristics of float glass surfaces, Journal of Non-Crystalline Solids. 19 (1975) 213–220. https://doi.org/10.1016/0022-3093(75)90086-1.

[19]   E. Guadagnino, O. Corumluoglu, Indirect determination of sulphide sulphur in glass by flame atomic absorption spectrometry: Report of ICG/TC 2 "chemical durability and analysis," Glass Technology. 38 (1997) 179–182.

[20]   T. Sato, Y. Takahashi, K. Yabe, An X-Ray Emission Spectroscopic Investigation of the Chemical Bond of Sulfur. I. The Peak Shift of K α and the Number of Valence Electrons of the Sulfur Atom in Compounds , Bull Chem Soc Jpn. 40 (1967) 298–301. https://doi.org/10.1246/bcsj.40.298.

[21]   A. Faessler, M. Goehring, Röntgenspektrum und Bindungszustand - Die Kα-Fluoreszenzstrahlung des Schwefels, Naturwissenschaften. 39 (1952) 169–177. https://doi.org/10.1007/BF00589801.

[22]   Y. Gohshi, O. Hirao, I. Suzuki, Chemical State Analyses of Sulfur, Chromium and Tin by High Resolution X-Ray Spectrometry, Advances in X-Ray Analysis. 18 (1974) 406–414. https://doi.org/10.1154/s0376030800006911.

[23]   M.E. Fleet, X. Liu, S.L. Harmer, H.W. Nesbitt, Chemical state of sulfur in natural and synthetic lazurite by S K-edge xanes and X-ray photoelectron spectroscopy, Canadian Mineralogist. 43 (2005) 1589–1603. https://doi.org/10.2113/gscanmin.43.5.1589.

[24]   R. Alonso Mori, E. Paris, G. Giuli, S.G. Eeckhout, M. Kavčič, M. Žitnik, K. Bučar, L.G.M. Pettersson, P. Glatzel, Electronic structure of sulfur studied by X-ray absorption and emission spectroscopy, Analytical Chemistry. 81 (2009) 6516–6525. https://doi.org/10.1021/ac900970z.

[25]   M. Wilke, K. Klimm, S.C. Kohn, Spectroscopic studies on sulfur speciation in synthetic and natural glasses, Reviews in Mineralogy and Geochemistry. 73 (2011) 41–78.

https://doi.org/10.2138/rmg.2011.73.3.

[26]   K. Klimm, R.E. Botcharnikov, The determination of sulfate and sulfide species in hydrous silicate glasses using Raman spectroscopy, American Mineralogist. 95 (2010) 1574–1579. https://doi.org/10.2138/am.2010.3590.
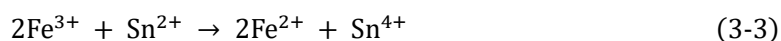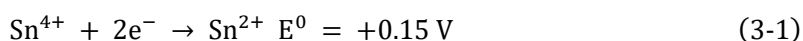
Chapter3

Speciation of Tin Ions in Oxide Glass Containing Iron Oxide through Solvent Extraction and Inductively Coupled Plasma Atomic Emission Spectrometry after the Decomposition Utilizing Ascorbic Acid

3.1 Introduction

Glass is a versatile material used in a wide variety of industries. The incorporation of trace elements into glass can alter its color, optical, and manufacturing properties. Tin oxide is used in trace quantities as a color modifier for gold and copper ruby glass[1], a fluorescent agent[2], and a fining agent[3,4]. These processes are based on reduction-oxidation reactions. Determining the concentrations of Sn^{2+} and Sn^{4+} in glass is important, and a reliable method is required. Methods for determining Sn valence in glass can typically be divided into wet chemical and physical analyses.

Examples of wet chemical analysis include titration[5] and spectrophotometric methods[6]. These methods can be performed daily in laboratories, and the common advantages of wet chemical analysis are better precision, lower detection limit, and lower cost[7]. However, a major drawback of wet chemical analysis of glass materials for valence speciation is the change in the valence of the target element during decomposition using hydrofluoric acid. Generally, an inert atmosphere can prevent the oxidation of species by air during sample decomposition[8–10]. The other possible valence change can be caused by the redox reaction with other multivalent elements. Fe is a multivalent element that causes the redox reaction with Sn due to the standard potential energy of the following reactions:

$$Sn^{4+} + 2e^- \rightarrow Sn^{2+} \quad E^0 = +0.15\,V \qquad (3\text{-}1)$$

$$Fe^{3+} + e^- \rightarrow Fe^{2+} \quad E^0 = +0.77\,V \qquad (3\text{-}2)$$

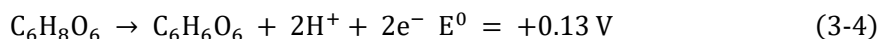$$2Fe^{3+} + Sn^{2+} \rightarrow 2Fe^{2+} + Sn^{4+} \qquad (3\text{-}3)$$

Industrial glass often contains Fe either due to a deliberate addition of Fe-containing raw materials, or as an unavoidable impurity in other added raw materials[11,12]. The previously reported methods[5,6] are not suitable for industrially manufactured glass materials due to the redox reaction (Equation 3) that occurs during decomposition using hydrofluoric acid. In the previously reported methods, redox reactions were not considered[5] or iron-free glass materials synthesized in the laboratory were used[6].

Examples of physical analysis are Mössbauer spectroscopy[13–17], X-ray absorption fine structure (XAFS)[18–20], high-resolution X-ray fluorescence analysis (HR-XRF)[21,22], and X-ray photoelectron spectroscopy (XPS)[23]. A common advantage of physical analysis is elemental selectivity as the interference from other elements, including Fe, is small or negligible. However, these methods have limitations. XAFS requires the use of synchrotron radiation facilities, and its routine use is challenging. One of the drawbacks of HR-XRF is the low signal-to-noise ratio owing to its two-crystal system. Additionally, this equipment is not widely used, and a long analysis time is required to obtain a sufficient signal-to-noise ratio for glass materials that contain trace amounts of Sn. Another drawback is that HR-XRF requires either reference materials, or a different method to determine the concentration of total Sn to obtain the concentrations of Sn^{2+} and Sn^{4+}. The drawbacks of XPS include the analysis depth and sensitivity. The analysis depth is less than 10 nm, which is too shallow to determine the Sn valence for the bulk of the sample. XPS usually requires more than 1 mass% of Sn to determine the precise valence state.

As mentioned above, both wet chemical and physical analyses have advantages and disadvantages. Wet chemical analysis is the preferred method to routinely analyze and determine the presence of Sn in glass, but faces challenges in determining the concentration of different Sn valences. Therefore, this study aims to propose, demonstrate, and validate a novel wet chemical analysis method for Sn

speciation in glass containing iron oxide. The first challenge is to maintain the valence of Sn during wet analysis while preventing the redox reaction between Sn^{2+} and Fe^{3+}. There are several possible approaches: a kinetic approach that slows down the redox reaction and virtually eliminates the reaction[24], masking Fe^{3+} [25], and expelling Fe^{3+} from the system[26] before causing the redox reaction. In this study, we added a reducing agent to reduce Fe^{3+}, thereby preventing the redox reaction between Sn^{2+} and Fe^{3+}. The selected reducing agent was ascorbic acid ($C_6H_8O_6$), a well-known reducing agent for Fe^{3+} (Equations 4 and 5). The redox reaction between ascorbic acid and Fe^{3+} occurs readily at pH 1.5 or lower and ascorbic acid does not cause any redox reaction with Sn[27].

$$C_6H_8O_6 \rightarrow C_6H_6O_6 + 2H^+ + 2e^- \quad E^0 = +0.13\,V \tag{3-4}$$

$$2Fe^{3+} + C_6H_8O_6 \rightarrow 2Fe^{2+} + C_6H_6O_6 + 2H^+ \tag{3-5}$$

The second challenge is to separately measure the concentration of each valence of Sn, namely Sn^{2+} and Sn^{4+}. Several possible approaches exist: coloring either ion and subsequently measuring the concentration by using a colorimetric method[8,9]; separating either ion by using a volatilization separation method and measuring the concentration[10]; separating each ion by using a solvent extraction method. A solvent extraction method utilizing diethyldithiocarbamate (DDTC) was used since it selectively extracts Sn^{2+} to an organic phase[28] at pH values ranging from 1 to 2.2[29]. Considering the above two points, a mixture of ascorbic acid, hydrofluoric acid, and hydrochloric acid, which was adjusted to a suitable pH, was used to decompose the glass samples, prevent the redox reaction between Sn^{2+} and Fe^{3+} and separate Sn^{2+} and Sn^{4+} by the solvent extraction method using DDTC. The concentrations of Sn in the glass samples were found to be too low to be determined by the colorimetry method[28]; therefore, inductively coupled plasma atomic emission spectrometry (ICP-AES) was used to determine Sn^{4+} and total Sn in the liquid phase. Sn^{2+} was calculated by subtracting Sn^{4+} from the total Sn concentration. The proposed method was validated by comparing the average concentration of Sn valences obtained by Mössbauer spectroscopy for the prepared soda

58

lime silicate glass materials doped with tin oxide and iron oxide.

3.2 Experimental

3.2.1 Material Preparation

The glass studied had the following standard soda lime silicate glass mass% composition: $16.5Na_2O \cdot 9.4CaO \cdot 74.1SiO_2$. They were produced by melting from raw materials of Na_2CO_3, $CaCO_3$, and SiO_2 and doped with 0.5 mass% SnO_2, 0-0.05 mass% Fe_2O_3, and 0-0.5 mass% carbon, as a reducing reagent, using a platinum crucible at 1500 °C. Table 3-1 lists the sample names and dopant concentrations used. The samples were then cut and mirror-polished using cerium oxide. A glass standard reference material, SRM 1830 (National Institute of Standards and Technology, Gaithersburg, USA), was used to confirm the effect of Fe^{3+}. Table 3-2 lists the certified compositions. The concentration of Fe^{3+} in SRM 1830 was calculated from the certified composition of total Fe and Fe^{2+}.

Table 3-1 Sample names and the concentrations of dopants used given in mass%

Sample name	SLS-M01	SLS-M02	SLS-M03	SLS-M04
SnO_2	0.50	0.50	0.50	0.50
Fe_2O_3	-	0.05	-	0.05
C	-	-	0.50	0.50

Table 3-2 Certified compositions of the glass reference material (SRM 1830) given in mass%. Values after the plus-minus sign indicate 95% confidence intervals

	SRM 1830		
SiO_2	73.07	±	0.04
Na_2O	13.75	±	0.06
CaO	8.56	±	0.06
MgO	3.90	±	0.04
Al_2O_3	0.12	±	0.02
K_2O	0.04	±	0.01
SO_3	0.26	±	0.01
Fe_2O_3(total)	0.121	±	0.003
FeO	0.032	±	0.004
TiO_2	0.011	±	0.001

3.2.2 Apparatus and instrumentation

A wavelength-dispersive X-ray fluorescence spectrometer (ZSX Primus II, Rigaku Corporation, Tokyo, Japan) was used to measure the compositions of produced samples. A 120 mL polytetrafluoroethylene (PTFE) decomposition vessel was used to decompose the glass samples with reagents. A magnetic stirrer and a 40×7 mm^2 stirring bar were used to stir the samples and reagents in the vessel. A 100 mL polypropylene separatory funnel with a stop valve was used to add reagents to the vessel. A 100 mL glass separatory funnel was used to extract Sn^{2+} into the organic phase. A 50 mL volumetric flask was used to fill the sample solutions. A 10 mL syringe (Terumo Corporation, Tokyo, Japan) and a syringe filter with 0.45 μm pore (Toyo Roshi Kaisya, Ltd., Tokyo, Japan) were

used to transfer sample solutions and to remove any unexpected solids. An inductively coupled plasma atomic emission spectrometer (SPS5520, Hitachi High-Tech Corporation, Tokyo, Japan) was used to determine the Sn concentration.

3.2.3   Reagents and chemicals

Hydrofluoric acid (HF, 50 mass%), hydrochloric acid (HCl, 36 mass%) of atomic absorption spectrometry grade, boric acid ascorbic acid, mixed xylene (Kanto Chemical Co., Inc., Tokyo, Japan) of special grade, and diethylammonium diethyldithiocarbamate (FUJIFILM Wako Pure Chemical Corporation, Osaka, Japan) of Wako 1st grade were used. Standard solutions of Sn and Fe (1 g/L) of ion chromatography grade (Kanto Chemical Co., Inc., Tokyo, Japan) were used. Deionized water was degassed and used.

3.2.4   Composition analysis

The compositions of produced samples were measured by XRF using fundamental parameter procedures[30]. The X-ray tube for primary excitation was a rhodium anode X-ray tube with the exciting conditions of 50 kV and 60 mA, operated under vacuum conditions. The measurement area was 30mmφ. The SnO_2 concentrations of samples were determined by chemical analysis, as was done for the total Sn in this study. Details were presented in the next two sections.

3.2.5   Sn Speciation procedure

3.2.5.1   Decomposition of glass samples and the separation of Sn^{2+}

Fig. 3-1 shows the apparatus used for the decomposition of the glass samples. A 30 mg aliquot of the ground glass was accurately weighed in a PTFE decomposition vessel and moistened with 1 mL of 5 mass% ascorbic acid. A mixture of 10 mL of 1.4 mol/L HF and 0.12 mol/L HCl was added to the

polypropylene separatory funnel on the vessel, which was degassed by passing nitrogen through the solution for 2 min. This was done by twisting the stop valve and the three-way valve to expel oxygen in the solution. The decomposition vessel was purged by passing nitrogen through at approximately 10 mL/s for 5 min to remove oxygen in the solution. The degassing process and purging process are collectively named 'deoxidizing process'. The mixture of HF and HCl solution was added to the decomposition vessel by twisting the stop valve and the three-way stop valve. Glass samples were decomposed by stirring for 30 min with nitrogen flow at approximately 10 mL/s. A boric acid solution (10 mL, 4 mass%) was added to the polypropylene separatory funnel during decomposition. After decomposition, nitrogen gas was passed through the boric acid solution in the funnel for 2 min by twisting the stop valve and the three-way valve to expel oxygen in the solution. The solution was added to the decomposition vessel and stirred with the decomposition solution for 1 min to ensure safety; boric acid complexes with free HF to produce HBF_4[31], and the solution does not substantially dissolve glassware[32,33]. The vessel was opened, and the solution in the vessel was transferred to a 50 mL volumetric flask. A small amount of water was added to the vessel to wash it; the water was transferred to the same 50 mL volumetric flask, and the solution was diluted to 50 mL with water. The solution in the flask was named "solution A." Approximately 10 mL of solution A was sampled twice using a syringe. The 20 mL solution A sample was added with a syringe into a 100 mL glass separatory funnel containing 5 mL of xylene mixed with 0.1 mass% diethylammonium diethyldithiocarbamate. A syringe filter was used to remove any unexpected solids. The funnel was shaken for 1 min to extract Sn^{2+} in solution A into the organic phase. This procedure was performed twice. The water phase in the funnel was sampled, and the solution was named "solution B." These procedures were performed three times (n = 3) for each sample.
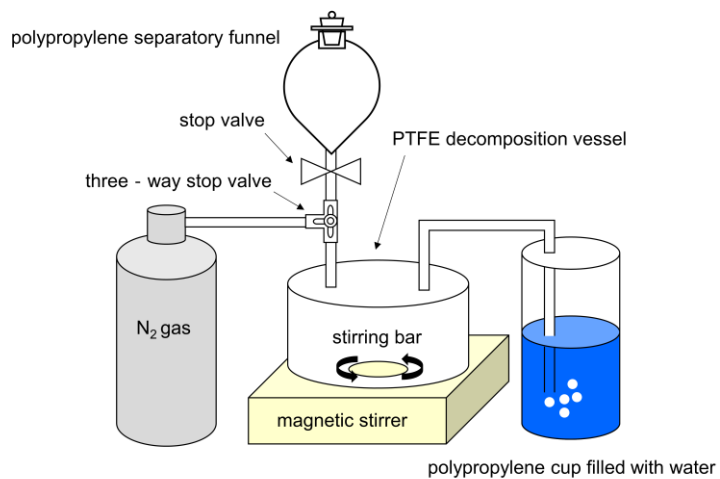
Fig. 3-1 Schematic representation of the experimental setup for decomposition of the glass samples. Glass samples are decomposed in the PTFE decomposition vessel with nitrogen flow. The nitrogen flow in the vessel is confirmed by the presence of nitrogen bubbles in a polypropylene cup filled with water.

3.2.5.2　Determination of Sn

The concentrations of Sn present in solutions A and B, which contain total Sn and Sn^{4+}, respectively, were determined by ICP-AES. Table 3-3 lists the measurement conditions of ICP-AES. The concentrations of total Sn, Sn^{4+}, and Sn^{2+} in the glass samples were calculated as follows:

In mass%

$$\text{Total Sn (as SnO}_2 \text{ mass\%)} = \frac{\text{Sn in solution A} \left(\frac{\mu g}{mL}\right) \times 50 \text{ (mL)}}{\text{Sample weight (mg)}} \times 10^{-1} \times 1.2696 \qquad (3\text{-}6)$$

$$\text{Sn}^{4+}(\text{as SnO}_2 \text{ mass\%)} = \frac{\text{Sn in solution B} \left(\frac{\mu g}{mL}\right) \times 50 \text{ (mL)}}{\text{Sample weight (mg)}} \times 10^{-1} \times 1.2696 \qquad (3\text{-}7)$$

$$\text{Sn}^{2+}(\text{as SnO}_2 \text{ mass\%)} = \text{Total Sn (as SnO}_2 \text{ mass\%)} - \text{Sn}^{4+}(\text{as SnO}_2 \text{ mass\%)} \qquad (3\text{-}8)$$

In mmol/g

$$\text{Total Sn} \left(\text{as Sn} \frac{mmol}{g}\right) = \frac{\text{Sn in solution A} \left(\frac{\mu g}{mL}\right) \times 50 \text{ (mL)}}{\text{Sample weight (mg)}} \times 10^2 \div 118.71 \left(\frac{g}{mol}\right) \qquad (3\text{-}9)$$

$$\text{Sn}^{4+} \left(\text{as Sn} \frac{mmol}{g}\right) = \frac{\text{Sn in solution B} \left(\frac{\mu g}{mL}\right) \times 50 \text{ (mL)}}{\text{Sample weight (mg)}} \times 10^2 \div 118.71 \left(\frac{g}{mol}\right) \qquad (3\text{-}10)$$

$$\text{Sn}^{2+} \left(\text{as Sn} \frac{mmol}{g}\right) = \text{Total Sn} \left(\text{as Sn} \frac{mmol}{g}\right) - \text{Sn}^{4+} \left(\text{as Sn} \frac{mmol}{g}\right) \qquad (3\text{-}11)$$

The concentrations were calculated as SnO_2 mass% following the conventions for describing the composition of oxide glass, and as Sn mmol/g to calculate the redox reaction between Sn^{2+} and Fe^{3+}. Equations 6 and 7 show the conversion factor, 1.2696, from Sn to SnO_2. Equations 9 and 10 show the atomic weight of Sn, 118.71 g/mol. In this study, the ratio of Sn^{2+} to total Sn is defined as the Sn redox, indicating the degree of reduction, as follows:

$$\text{Sn redox (\%)} = \frac{Sn^{2+}(\text{as } SnO_2 \text{ mass\%})}{\text{Total Sn (as } SnO_2 \text{ mass\%})} \times 100 = \frac{Sn^{2+}\left(\text{as Sn} \frac{\text{mmol}}{\text{g}}\right)}{\text{Total Sn }\left(\text{as Sn} \frac{\text{mmol}}{\text{g}}\right)} \times 100 \quad (3\text{-}12)$$

Table 3-3 ICP-AES measurement conditions.

RF power	1.2 kW
Plasma gas flow	15.0 L/min
Auxiliary gas flow	1.5 L/min
Nebulizer gas pressure	0.75 MPa
Emission line	Sn(II): 189.927 nm

3.2.5.3 Blank test

A blank test was conducted throughout the entire procedure, consisting of the decomposition, separation, and determination procedures. The test was repeated four times to calculate the mean blank value and the standard deviation (σ). The limit of detection was defined as the mean blank value plus 3σ. The limit of quantification was defined as the mean blank value plus 10σ.

3.2.6 Validation of the method

3.2.6.1 The effect of Fe^{3+}

To validate the proposed method, the effect of Fe^{3+} on the proposed method was also investigated. A 30 mg aliquot of ground SRM 1830 was added before 30 mg of SLS-M03 was decomposed to confirm the effect of Fe^{3+} in SRM 1830 on the obtained Sn redox value. Because SRM 1830 contains Fe^{3+}, if the redox reaction between Fe^{3+} in SRM 1830 and Sn^{2+} in SLS-M03 occurs (Equation 3-3), the obtained Sn redox value decreases as compared to that of SLS-M03. If the proposed method can prevent the redox reaction (Equation 3-3), the obtained Sn redox value would be the same as that of SLS-M03. The test was repeated twice (n = 2).

Various amounts of Fe^{3+} (0.12 mol% HCl solution), ranging from 0.42 to 8.4 μmol, were added before 30 mg SLS-M03 was decomposed. Ascorbic acid was not added to the iron containing solution, preventing Fe^{3+} to be reduced to Fe^{2+}, to confirm the effect of Fe^{3+}. Other conditions were kept the same as those described in Section 3.2.5.1.

3.2.6.2 The effects of addition of ascorbic acid, and the deoxidizing process

The effects of addition of ascorbic acid, and the deoxidizing process were tested using sample SLS-M04. The tests were performed with and without the addition of ascorbic acid, each scenario tested in combination with and without the deoxidizing process. Other conditions were kept the same as those described in Section 3.2.5.1.

3.2.7 Mössbauer spectroscopy measurement

The valence states of Sn in the glass samples were measured by ^{119}Sn spectroscopy using standard transmission geometry. Gamma rays (γ-rays) emitted from $Ca^{119m}SnO_3$ were used. The Doppler velocity range of the source was ±8 mm/s. The velocity scale was calibrated using a $^{57}CoRh$ source and a standard α-Fe foil absorber. The velocity 0 mm/s criterion was set to the peak position of the

CaSnO$_3$ (Sn^{4+}) standard material. A Pd 50 μm foil was used as a filter to cut the interfering Sn-Kα X-rays emitted from the Sn source. A NaI scintillation counter was used for γ-ray detection. The source activity was 444–416 MBq (12.0–11.2 mCi). The ^{119}Sn Mössbauer spectra at room temperature were measured for all glass samples in plate form. The Mössbauer spectra of ^{119}Sn of a sample material doped with 0.5 mass% SnO$_2$ and 0.5 mass% carbon were measured in a flow-type cryostat at four temperatures (78 K, 100 K, 200 K, and 300 K). The obtained spectra were deconvoluted using Lorentzian curves. For the oxidized atmosphere samples (SLS-M01, SLS-M02), the spectra were deconvoluted using one set of quadrupole-split doublet corresponding to Sn^{4+}, and one set of quadrupole-split doublet corresponding to Sn^{2+}. For the reduced atmosphere samples (SLS-M03, SLS-M04), the spectra were deconvoluted using one set of quadrupole-split doublet corresponding to Sn^{4+} and two sets of quadrupole-split doublet corresponding to Sn^{2+}. The Debye temperature of the Sn^{2+} and Sn^{4+} sites were obtained from the slope of the straight line in the relationship between the temperature and the logarithm of the integral absorption intensities for the sample material doped with 0.5 mass% SnO$_2$ and 0.5 mass% carbon, by applying the high-temperature approximation formula of the Debye model:

$$\ln f = -\frac{6E_R}{k_B \theta_D^2} \times T \qquad (3\text{-}13)$$

$$E_R = \frac{E_\gamma^2}{2Mc^2} \qquad (3\text{-}14)$$

$$A = \text{const} \times f \qquad (3\text{-}15)$$

Here, f represents the recoilless fraction, θ_D is the Debye temperature of the Mössbauer ion, E_R is the recoil energy, k_B is the Boltzmann constant, T is the measurement temperature, E_γ is the energy of Mössbauer γ-rays (23.87 keV), M is the mass of the recoil nucleus (M(Sn) = 118.90331 u), c is the velocity of light, and A is the integral absorption intensity. Assuming the Debye temperature obtained for the sample material doped with 0.5 mass% SnO$_2$ and 0.5 mass% carbon is the same for all samples,

the integral absorption intensities obtained for each sample at room temperature were corrected by the recoilless fraction to obtain the atomic presence ratios of Sn^{2+} and Sn^{4+}.

3.3 Results and discussions

3.3.1 Sample composition

Table 3-4 lists composition of each sample determined by XRF and chemical analysis. The compositions were close to the target values except for SnO_2. In all the samples, the concentrations of total Sn were lower than the doped concentrations (0.5 mass%). It is highly possible that Sn volatilized as SnO during melting. A small amount of Al_2O_3 was found as a result of impurities from the raw materials or the experimental environment.

Table 3-4 Composition of each glass sample measured by XRF and chemical analysis (given in mass%).

	SLS-M01	SLS-M02	SLS-M03	SLS-M04
SiO_2	73.6	73.6	73.6	73.6
Al_2O_3	0.10	0.11	0.13	0.12
Na_2O	16.4	16.4	16.4	16.4
CaO	9.33	9.31	9.33	9.33
SnO_2	0.40	0.40	0.33	0.34
Fe_2O_3	0.02	0.06	0.02	0.07

3.3.2 Detection limit and quantification limit of the proposed method

The mean blank value, detection limit, and quantification limit of the three Sn valences are the following: for Sn^{4+}, <0.0001, <0.0001, and 0.004 mass%; for total Sn, <0.0001, 0.001, and 0.003

mass%; for Sn^{2+}, 0.001, 0.002, and 0.004 mass%.

3.3.3 Determination of Sn^{2+} and Sn^{4+} in glass samples by the proposed method

Table 3-5 lists the concentrations of total Sn, Sn^{4+}, and Sn^{2+} in glass samples in the form of tin dioxides. It also lists the Sn redox, indicating the degree of reduction as the ratio of Sn^{2+} to total Sn. The repeatability of n = 3 was good. The Sn redox values of SLS-M03 and SLS04 were higher than those of SLS-M01 and SLS-M02, reflecting the melting conditions. SLS-M03 and SLS-M04 were produced by melting with carbon; on the other hand, SLS-M01 and SLS-M02 were produced by melting without carbon. Table 3-6 lists the average concentrations of total Sn, Sn^{4+} and Sn^{2+} in glass samples in form of mmol/g as well.

It took approximately 1 h to complete the decomposition and separation of one sample. This method can analyze up to 6-8 samples per day. More samples can be treated by increasing the number of apparatus. It took approximately 1 h to determine the Sn content of samples using ICP-AES. Since the solutions were stable for a couple of days, samples can be stored, and ICP-AES analysis can be conducted at a later stage.

Table 3-5 Concentrations of total Sn, Sn^{4+} and Sn^{2+} in the glass samples given in mass% of tin dioxides, as well as the calculated Sn redox.

		Total Sn (as SnO_2 mass%)	Sn^{4+} (as SnO_2 mass%)	Sn^{2+} (as SnO_2 mass%)	Sn redox (%)
SLS-M01	n = 1	0.406	0.367	0.039	9.6
	n = 2	0.391	0.351	0.040	10
	n = 3	0.404	0.366	0.038	9.4
	Avg.	0.400	0.361	0.039	9.8
SLS-M02	n = 1	0.403	0.382	0.021	5.2
	n = 2	0.390	0.368	0.022	5.6
	n = 3	0.416	0.392	0.024	5.8
	Avg.	0.403	0.381	0.022	5.5
SLS-M03	n = 1	0.317	0.090	0.227	72
	n = 2	0.350	0.086	0.264	75
	n = 3	0.333	0.085	0.248	74
	Avg.	0.334	0.088	0.246	74
SLS-M04	n = 1	0.333	0.080	0.253	76
	n = 2	0.344	0.084	0.260	76
	n = 3	0.341	0.086	0.255	75
	Avg.	0.339	0.083	0.256	76

Table 3-6 Concentrations of total Sn, Sn^{4+}, and Sn^{2+} in the glass samples given in mmol/g.

	Total Sn	Sn^{4+}	Sn^{2+}
	(mmol/g)	(mmol/g)	mmol/g
SLS-M01	2.66	2.40	0.26
SLS-M02	2.67	2.52	0.15
SLS-M03	2.21	0.58	1.63
SLS-M04	2.25	0.55	1.70

3.3.4   Effect of Fe^{3+}

The Sn redox results of SLS-M03 decomposed with SRM 1830 for n = 1 and n = 2 were both 74 %. The concentration of Fe^{3+} in SRM 1830, calculated from the certified values of total Fe and Fe^{2+}, was 1.07 mmol/g. The concentration of total Sn and Sn^{2+} in SLS-M03 was 2.21 and 1.63 mmol/g, respectively. Thus, the Sn redox should decrease by 24 % if the redox reaction between Fe^{3+} in SRM 1830 and Sn^{2+} in SLS-M03 occurs (Equation 3-3). The resulting Sn redox of SLS-M03 decomposed with SRM 1830, which is equal to the Sn redox of SLS-M03, as shown in Table 3-5, indicating that the proposed method fully prevented the redox reaction between Sn^{2+} and Fe^{3+} during decomposition. The ascorbic acid completely reduced Fe^{3+} in SRM 1830. This is because the reaction between ascorbic acid and Fe^{3+} occurs readily[27].

Table 3-7 shows the Sn redox of SLS-M03 solution with added Fe^{3+} with and without the addition of ascorbic acid. It also shows the Sn redox with the standard condition in Table 3-5 as reference. When Fe^{3+} was added without the addition of ascorbic acid, the Sn redox decreased. This indicates that the reaction of Equation 3-3 occurred during decomposition, as expected. Conversely, the Sn redox did not decrease quantitatively with respect to the amount of Fe^{3+} added. It is highly possible that the reaction rate of Equation 3-3 is relatively slow and does not proceed to completion during the reaction

time of this experimental condition.

Table 3-7 Sn redox of SLS-M03 with Fe^{3+} added in various amounts.

Addition of ascorbic acid	yes	no	no	no	no	no
Fe^{3+}(µmol)	0	0	0.42	0.84	1.68	8.42
Fe^{3+} mol ratio to Sn^{2+}	0	0	1	2	4	20
Sn Redox of SLS-M03(%)	75*	68	55	56	50	<2

*Standard condition

3.3.5   The effects of addition of ascorbic acid, and the deoxidizing process

Table 3-8 shows the Sn redox of SLS M-04 with and without the addition of ascorbic acid, with and without the deoxidizing process. It also shows the Sn redox with the standard condition in Table 3-5 as reference. Under the conditions where ascorbic acid was added, and the deoxidizing process was not employed, the Sn redox was lower than the standard condition. It is considered that the dissolved oxygen in the solution caused the oxidation of Sn^{2+}. From the above results, it was found that ascorbic acid acts as a reducing agent for Fe^{3+}, counteracts the redox reaction between Fe^{3+} and Sn^{2+}, and prevents the oxidation of Sn^{2+} by dissolved oxygen.

Table 3-8 Sn redox of SLS M-04 calculated with and without the addition of ascorbic acid, with and without degassing/N₂ purging.

Addition of ascorbic acid	yes	yes	no	no
Addition of the deoxidizing process	yes	no	yes	no
Sn redox of SLS M-04(%)	75*	60	63	44

*Standard condition

3.3.6   Valence analysis result by Mössbauer spectroscopy

Table 3-9 lists the Sn redox measured by Mössbauer spectroscopy corrected with the recoilless fractions at room temperature (300 K). The Mössbauer spectra of the glass samples at room temperature (300 K) is shown in Fig. 3-2. Two absorption doublets were observed to be centered at isomer shifts of ~ 0 and 2.8 mm/s. The absorption at ~ 0 mm/s can be attributed to Sn^{4+} and that at ~ 2.8 mm/s to Sn^{2+}, according to previous reports[34–36]. The spectra of SLS-M03 and SLS04, where 0.5 mass% carbon was added, show obvious Sn^{2+} peaks. Because the peaks of the two sets of Sn^{2+} doublets were connected continuously, it was difficult to deconvolute uniquely. However, it was confirmed that the total Sn^{2+} ratio did not depend on the deconvolution method. The Mössbauer spectra of SLS-M03 at several temperatures is shown in Fig. 3-3. The lower the measurement temperature, the larger is the Sn^{2+} peak. Fig. 3-4 shows the relationship between the logarithm of the integrated absorption intensity of the Mössbauer spectra of Sn^{2+} and Sn^{4+} of SLS-M03 and the measurement temperatures. The calculated Debye temperatures were 185 and 266 K for Sn^{2+} and Sn^{4+}, respectively. These results are in good agreement with those of previously researched soda lime silicate glass[16,17]. The recoilless fractions for Sn^{2+} and Sn^{4+} of SLS-M03 at each temperature calculated from the Debye temperature are listed in Table 3-10.

Table 3-9 Sn redox measured by Mössbauer spectroscopy corrected with the recoilless fraction at room temperature (300 K).

|	Sn Redox (%)
SLS-M01	11
SLS-M02	5.2
SLS-M03	73
SLS-M04	77
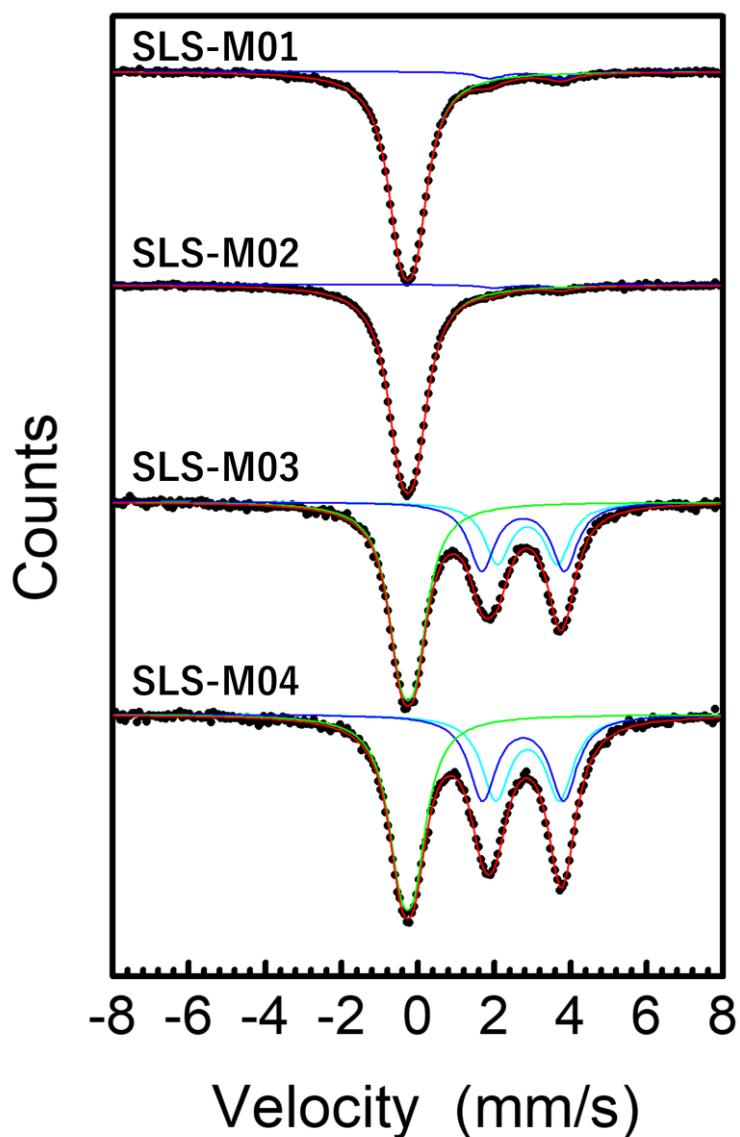
Fig. 3-2 Mössbauer spectra of glass samples with standard soda lime silicate glass mass% composition 16.5Na₂O·9.4CaO·74.1SiO₂, doped with 0.5 mass% SnO₂ at room temperature (300K). Red line shows the fitting result of the measurement result (black circles). Green line shows the fitting result of Sn^{4+}. Blue and light blue lines show the fitting results of Sn^{2+}. Because the peaks of the two sets of Sn^{2+} doublets of SLS-M03 and SLS-M04 are connected continuously, it is difficult to deconvolute them uniquely, as discussed in the text.
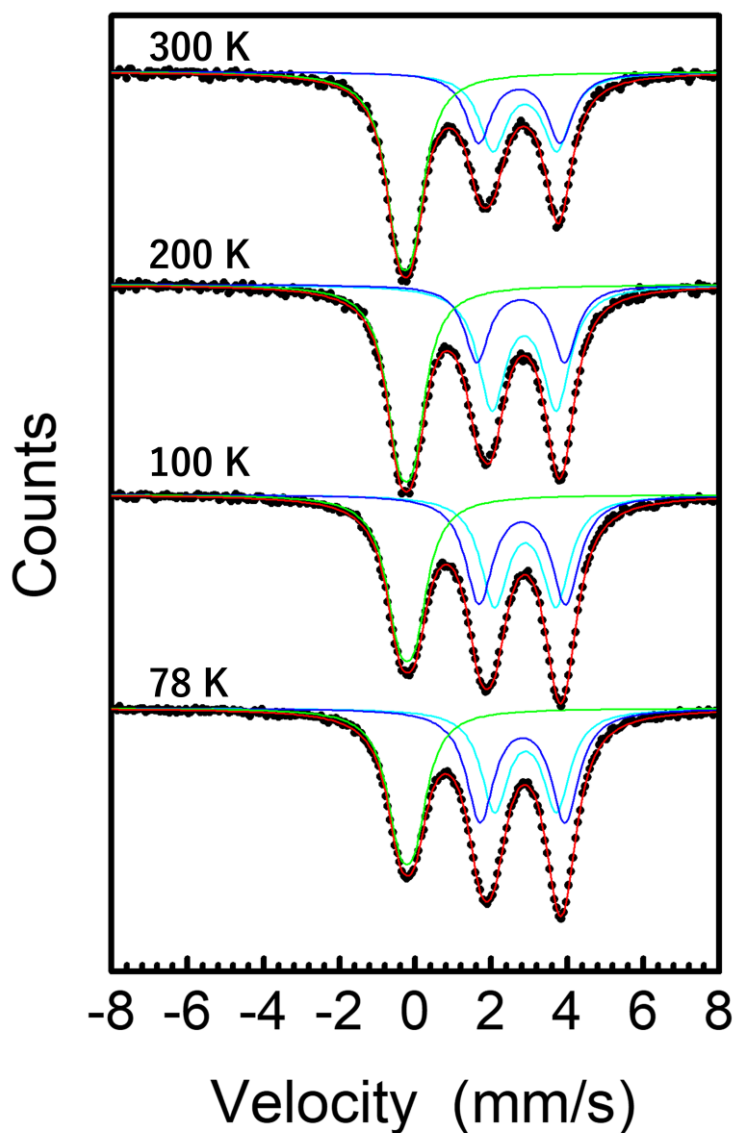
Fig. 3-3 Mössbauer spectra of SLS-M03 at several temperatures, with standard soda lime silicate glass mass% composition $16.5Na_2O \cdot 9.4CaO \cdot 74.1SiO_2$, doped with 0.5 mass% SnO_2 and 0.5 mass% carbon. Red line shows the fitting result of the measurement result (black circles). Green line shows the fitting result of Sn^{4+}. Blue and light blue lines show the fitting results of Sn^{2+}. Because the peaks of the two sets of Sn^{2+} doublets are connected continuously, it is difficult to deconvolute them uniquely, as discussed in the text.
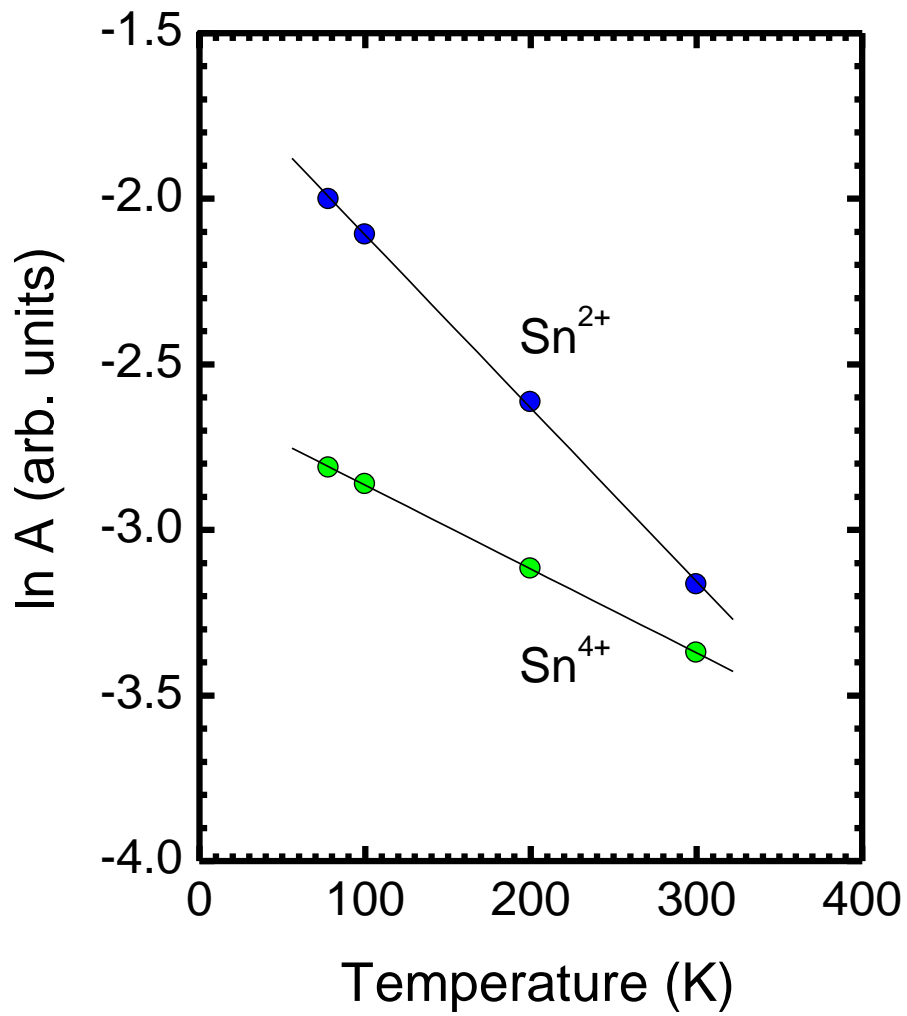
Fig. 3-4 Relationship between the measurement temperature and the integrated absorption intensity of Mössbauer spectra of Sn^{2+} and Sn^{4+} of SLS-M03 shown on a logarithmic scale.

Table 3-10 Recoilless fraction (*f*) for Sn^{2+} and Sn^{4+} of SLS-M03 at each measurement temperature as calculated from the Debye temperatures.

T(K)	Recoilless fraction (*f*)	
	Sn^{2+}	Sn^{4+}
300	0.21	0.47
200	0.35	0.60
100	0.59	0.78
78	0.67	0.82

3.3.7   Comparison of the results of the proposed method with Mössbauer spectroscopy

Fig. 3-5 shows a comparison of the Sn redox obtained through Mössbauer spectroscopy and the proposed method. The error bar of the x-axis is 2 % for Mössbauer spectroscopy, and the error bar of the y-axis is 1 σ for the proposed method. The results were in good agreement, including the results of the samples containing iron oxide. This confirms that the proposed method determines the Sn redox accurately.
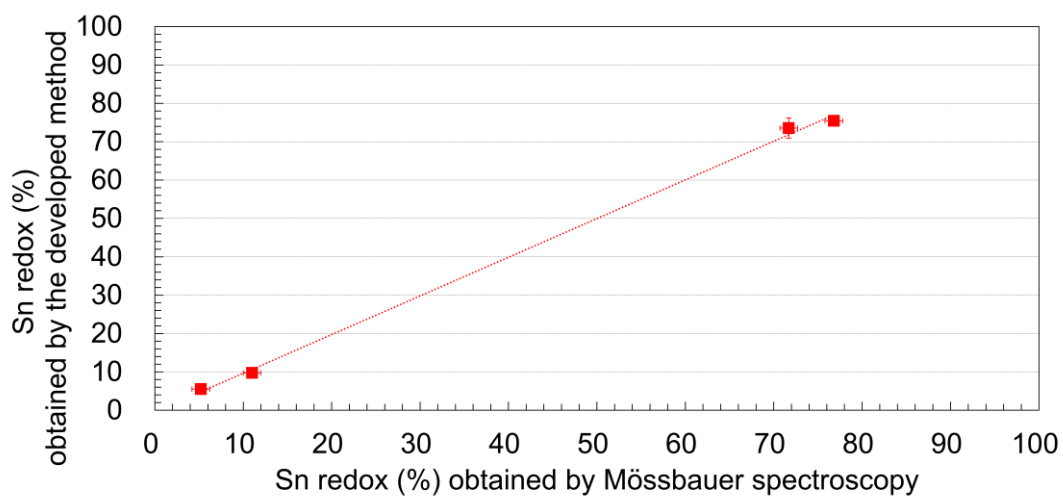
Fig. 3-5 Comparison of the Sn redox obtained by Mössbauer spectroscopy and the proposed method. The values measured by Mössbauer spectroscopy were corrected with the recoilless fractions at room temperature (300 K).

3.4　Conclusions

The present study investigates a novel wet chemical analysis method for determining the concentrations of trace total Sn and Sn^{4+} in oxide glass materials containing iron oxide. The method entails decomposing a glass sample, separating, and determining Sn^{4+} and total Sn concentrations. Sn^{2+} was calculated using total Sn and Sn^{4+}. The ratio of Sn^{2+} to total Sn (the Sn redox) were calculated. Glass samples were decomposed in a decomposition vessel with a mixture of ascorbic acid, hydrochloric acid, and hydrofluoric acid under a nitrogen purge. Ascorbic acid performed as a reducing agent for Fe^{3+}. Additionally, ascorbic acid inhibited the oxidation of Sn^{2+} by dissolved oxygen. Sn^{2+} was separated from the glass-decomposed solution into the organic phase as a diethyldithiocarbamate complex. ICP-AES was used to determine the concentrations of Sn^{4+} and total Sn. As sample materials, soda lime silicate glasses were doped with tin oxide and iron oxide. The Sn redox were compared to those obtained using Mössbauer spectroscopy, and were found to be in excellent agreement. Thus, the proposed approach holds significant promise for routine analytical studies of glass materials without the drawbacks associated with the industry's current standard methodologies.

3.5   References

[1]   S.D. Stookey, Coloration of glass by gold, silver, and copper, Journal of the American Ceramic Society. 32 (1949) 246–249. https://doi.org/10.1111/j.1151-2916.1949.tb18957.x.

[2]   L. Skuja, Isoelectronic series of twofold coordinated Si, Ge, and Sn atoms in glassy SiO_2: a luminescence study, Journal of Non-Crystalline Solids. 149 (1992) 77–95. https://doi.org/10.1016/0022-3093(92)90056-P.

[3]   K. Kim, Fining behavior in alkaline earth aluminoborosilicate melts doped with As_2O_5 and SnO_2, Journal of the American Ceramic Society. 96 (2013) 781–786. https://doi.org/10.1111/jace.12188.

[4]   A. Ellison, I.A. Cornejo, Glass Substrates for Liquid Crystal Displays, International Journal of Applied Glass Science. 1 (2010) 87–103. https://doi.org/10.1111/j.2041-1294.2010.00009.x.

[5]   J.S. Sieger, Chemical characteristics of float glass surfaces, Journal of Non-Crystalline Solids. 19 (1975) 213–220. https://doi.org/10.1016/0022-3093(75)90086-1.

[6]   R. Pyare, P. Nath, Simple and rapid spectrophotometric method for the determination of Tin(II) in binary alkali silicate glasses, Analyst. 110 (1985) 1321–1323. https://doi.org/10.1039/AN9851001321.

[7]   J.E. Amonette, J. Matyáš, Determination of ferrous and total iron in refractory spinels, Analytica Chimica Acta. 910 (2016) 25–35. https://doi.org/10.1016/j.aca.2015.12.024.

[8]   D.R.J. Jones, W.C. ansheski, D.S. Goldman, Spectrophotometric Determination of Reduced and Total Iron in Glass with 1,10-Phenanthroline, Analytical Chemistry. 53 (1981) 923–924. https://doi.org/10.1021/ac00229a049.

[9]   R. Akiyama, N. Kanno, Y. Suzuki, K. Yamamoto, Determination of ferrous and total iron at the surface of float glass by spectrophotometry combined with a stepwise etching technique, Glass Technology - European Journal of Glass Science and Technology Part A. 56 (2015) 37–

42.	https://www.ingentaconnect.com/content/sgt/gta/2015/00000056/00000002/art00001 (accessed November 24, 2021).

[10]	Y. Saijo, Y. Suzuki, M. Murata, R. Akiyama, M. Shimizu, Y. Shimotsuma, K. Miura, Separation and determination of sulfide sulfur and sulfate sulfur in soda lime silicate glass, Journal of Non-Crystalline Solids. 571 (2021) 121072. https://doi.org/10.1016/j.jnoncrysol.2021.121072.

[11]	Y. Arai, M. Inoue, K. Ishikawa, T. Yokote, Y. Kondo, K. Mori, Evolution of the glass light guide plate and its peripheral technologies for large size TV application, 2017. https://doi.org/10.1002/sdtp.11964.

[12]	H. Hijiya, Consideration on the structure of Fe^{2+} in system, NEW GLASS. 34 (2019) 14–17.

[13]	H. Masai, Y. Suzuki, T. Yanagida, K. Mibu, Luminescence of Sn^{2+} center in $ZnO-B_2O_3$ glasses melted in air and Ar conditions, Bull Chem Soc Jpn. 88 (2015) 1047–1053. https://doi.org/10.1246/bcsj.20150145.

[14]	D. Benne, C. Rüssel, M. Menzel, K.D. Becker, The effect of alumina on the Sn^{2+}/Sn^{4+} redox equilibrium and the incorporation of tin in $Na_2O/Al_2O_3/SiO_2$ melts, Journal of Non-Crystalline Solids. 337 (2004) 232–240. https://doi.org/10.1016/j.jnoncrysol.2004.04.017.

[15]	K.F.E. Williams, C.E. Johnson, J.A. Johnson, D. Holland, M.M. Karims, Mössbauer spectra of tin in binary SiSn oxide glasses, Journal of Physics: Condensed Matter. 7 (1995) 9485–9497.

[16]	K.F.E. Williams, C.E. Johnson, B.P. Tilley, D. Gelder, J.A. Johnson, Tin oxidation state, depth profiles of Sn^{2+} and Sn^{4+} and oxygen diffusivity in float glass by Mössbauer spectroscopy, Journal of Non-Crystalline Solids. 211 (1997) 164–172. https://doi.org/10.1016/S0022-3093(96)00636-9.

[17]	K.F.E. Williams, C.E. Johnson, O. Nikolov, M.F. Thomas, J.A. Johnson, J. Greengrass, Characterization of tin at the surface of float glass, Journal of Non-Crystalline Solids. 242 (1998) 183–188. https://doi.org/10.1016/S0022-3093(98)00799-6.

[18] H. Masai, T. Ina, S. Okumura, K. Mibu, Validity of Valence Estimation of Dopants in Glasses using XANES Analysis, Scientific Reports. 8 (2018) 415. https://doi.org/10.1038/s41598-017-18847-0.

[19] A.M. Flank, P. Lagarde, J. Jupille, H. Montigaud, Redox profile of the glass surface, Journal of Non-Crystalline Solids. 357 (2011) 3200–3206. https://doi.org/10.1016/j.jnoncrysol.2011.03.046.

[20] M. Zheng, H. Wang, T. Haizheng, H. Yourong, J. Hong, The effect of tin on sulfur K-edge X-ray absorption near edge structure spectra of soda-lime-silicate glass: An experimental and comparative study, Journal of Non-Crystalline Solids. 383 (2014) 71–74. https://doi.org/10.1016/j.jnoncrysol.2013.04.027.

[21] Y. Gohshi, O. Hirao, I. Suzuki, Chemical state analysis of sulfur, chromium and tin by high resolution X-ray spectrometry, Advanced in X-Ray Analysis. 18 (1974) 406–414. https://doi.org/10.1154/S0376030800006911.

[22] H. Masuda, Y. Fukumoto, K. Morinaga, Sn^{2+}/Sn^{4+} Redox Equilibrium in the Oxide Glasses, Interdisciplinary Graduate School of Engineering Sciences, Kyushu University. 14 (1992) 173–179. https://doi.org/10.15017/17267.

[23] L. Jie, X. Chao, XPS examination of tin oxide on float glass surface, Journal of Non-Crystalline Solids. 119 (1990) 37–40. https://doi.org/10.1016/0022-3093(90)90238-H.

[24] N. Kanno, M. Nakase, M. Harigai, Y. Saijo, R. Akiyama, K. Takeshita, The 35th Symposium on Ion Exchange & The 40th Symposium on Solvent Extraction, in: Approach to Determination of Fe^{2+}/Fe^{3+} in Sn^{2+} Containing Glass by Solvent Extraction, Kitakyusyu, 2021: p. 82.

[25] O. Corumluoglu, E. Guadagnino, Determination of ferrous iron and total iron in glass by a colorimetric method, Glass Technology. 40 (1999) 24–28.

[26] A. Frankenberger, R.R. Brooks, M. Hoashi, Determination of vanadium in steels and geological materials by liquid-liquid extraction and graphite furnace atomic absorption spectrometry, Analytica Chimica Acta. 246 (1991) 359–363. https://doi.org/10.1016/S0003-2670(00)80973-3.

[27] K. Mikami, Volumetric determination of iron by ascorbic acid method, The Journal of the Japan Society for Analytical Chemistry. 27 (1978) 160–164. https://doi.org/10.2116/bunsekikagaku.27.3_160.

[28] P.F. Wyatt, Diethylammonium Diethyldithiocarbamate for the Separation and Determination of Small Amounts of Metals Part II. The Isolation and Determination of Arsenic, Antimony and Tin in Organic Compounds, Analyst. 80 (1955) 368–379.

[29] H. Goto, Y. Kakita, Photometric Determination of Tin in Iron and Steel（III）. Photometric Method with Sodiumdiethyldithiocarbamate and its Application to the Deterrnination of Tin in Iron and Steel, Journal of the Japan Institute of Metals. 20 (1956) 319–322. https://doi.org/10.2320/jinstmet1952.20.6_319.

[30] P.J. Potts, A handbook of silicate rock analysis8, in: Blackie, Glasgow, 1987.

[31] P.J. Potts, A handbook of silicate rock analysis2, in: Blackie, Glasgow, 1987.

[32] B. Bernas, A New Method for Decomposition and Comprehensive Analysis of Silicates by Atomic Absorption Spectrometry, Analytical Chemistry. 40 (1968) 1682–1686. https://doi.org/10.1021/ac60267a017.

[33] D.E. Buckley, R.E. Cranston, Atomic absorption analyses of 18 elements from a single decomposition of aluminosilicate, Chemical Geology. 7 (1971) 273–284. https://doi.org/10.1016/0009-2541(71)90012-X.

[34] G.S. Collins, T. Kachnowski, N. Benczer-Koller, M. Pasternak, Application of the Mössbauer effect to the characterization of an amorphous tin-oxide system, Physical Review B. 19 (1979)

1369–1373. https://doi.org/10.1103/PhysRevB.19.1369.

[35] N. Kikuchi, A. Samizo, S. Ikeda, Y. Aiura, K. Mibu, K. Nishio, Carrier generation in a p -type oxide semiconductor: $Sn_2(Nb_{2-x}Ta_x)O_7$, Physical Review Materials. 1 (2017) 021601. https://doi.org/10.1103/PhysRevMaterials.1.021601.

[36] S. Miyasaka, T. Ishiyama, M. Nakano, K. Yanagihara, Y. Hayashi, T. Omata, Surface modification of soda–lime–silicate glass via the high-temperature electrochemical injection of tin ions, Applied Surface Science. 532 (2020) 147421. https://doi.org/10.1016/j.apsusc.2020.147421.

Chapter4

Speciation Analysis of Tin at the Tin Side of Float Glass by Solvent Extraction Combined with a Stepwise Etching Technique

4.1   Introduction

The float method is a mass-production technique used to form plate-shaped glass. In this method, molten glass is suspended over molten tin in a reducing atmosphere under a N_2/H_2 gas flow[1]. In addition to conventional soda lime silicate glass[1], high-quality glass, such as borosilicate glass[2], flat panel display glass[3], light guide plate glass[4], and glass for chemical strengthening,[5] is manufactured using this method. It is known that molten tin penetrates the glass surface that is in contact with the molten tin at the glass-tin interface (referred to as the tin side)[6], and this surface exhibits different properties from those of the glass-air interface (referred to as the atmosphere side)[7–12]. Achieving a high-quality glass surface requires a detailed understanding of the reaction between the glass surface and the molten tin. Previous studies have shown that tin that has penetrated the tin side reacts with polyvalent elements in the glass and exhibits a complex concentration and redox profile[6,13–16]. These profiles were explained using a diffusion-reaction model, as follows[8,10,13–15,17]:

a) When the glass melt enters the float chamber, atmospheric hydrogen passing through the molten tin penetrates the tin side [13], and Fe^{3+} and S^{6+} in the surface layer of the tin side are reduced to Fe^{2+} and S^{2-}. Accordingly, a reduced layer with no Fe^{3+} or S^{6+} ions was formed on the surface of the tin side. Sn^{2+} that can penetrate the tin side can be generated in two ways: by oxidation of molten tin (Sn^0) by a small amount of residual oxygen in the float chamber[13], or by the redox reaction between molten tin (Sn^0) and Fe^{3+} on the glass surface[10,15]. These Sn^{2+} ions penetrate the surface layer of the tin side

86

through an ion-exchange reaction between Sn^{2+} and two Na^+ ions or Fe^{2+}.

b) The Sn^{2+} that penetrates the surface of the tin side can diffuse deeper into the glass melt as a result of ion-exchange reaction[10,13,14,17]. Accordingly, the tin penetration exhibits a diffusion profile associated with the diffusion coefficient of Sn^{2+}.

c) Sn^{2+} that diffuses into the glass melt is oxidized to Sn^{4+} by redox reactions with Fe^{3+}[13–18] or S^{6+}[16] in deeper parts of the melt. Sn^{4+} then diffuses in accordance with its diffusion coefficient, which is smaller than that of Sn^{2+}[8]. Consequently, the reduced layer exhibits the diffusion profile of Sn^{2+} because of the absence of Sn^{4+} ions, whereas the deeper region shows a penetration profile corresponding to the diffusion coefficient of Sn^{4+}.

d) The total Sn concentration profile shows the convolution of the Sn^{2+} and Sn^{4+} profiles, which are identified as a satellite peak ("tin hump") at the interface of the reduced layer and the deeper region. Therefore, not only the total Sn concentration profile from the tin side but also the Sn redox profile of the glass surface is important.

The total Sn concentration profiles on the tin side have been studied using many conventional methods, such as electron probe microanalysis (EPMA)[6,10,16,19,20], X-ray fluorescence (XRF) analysis[18], secondary-ion mass spectrometry (SIMS)[13], X-ray photoelectron spectroscopy (XPS)[8,19,21], and Rutherford backscattering spectroscopy (RBS)[10,22].

Similarly, the Sn redox profile on the tin side has been studied, using transmission Mössbauer spectroscopy (TMS)[19,20,23], conversion-electron Mössbauer spectroscopy (CEMS)[10,14,15,17,20,24], and X-ray absorption fine structure (XAFS) using synchrotron radiation[16].

However, these methods for determining the Sn redox profile have some problems: they may be less quantitative, and involve restrictions on the use of equipment and facilities. In addition, techniques such as Mössbauer spectroscopy require a radiation-controlled area and accurate measurement of the

Debye temperature of each target ion to quantitatively determine the Sn redox. Multiple measurements must be carried out at different temperatures to accurately determine the Debye temperature, which in turn will lead to a long analysis time. Williams et al.[20] pointed out that the Debye temperature of Sn^{4+} on the outermost surface of the tin side of float glass differs from that of Sn^{4+} inside the glass. This indicated that the Debye temperature must be measured at each depth, which is virtually impossible. Additionally, the depth resolution of Mössbauer spectroscopy is not high. The highest depth resolution, 2 μm, is achieved using CEMS [20,25].

Flank et al.[16] showed an alternative method of depth profiling using XAFS, but this was not quantitative, and the outermost part of the sample was not clear because of the glue used in the sample preparation. However, the depth resolution was 1 μm, which is the best to date.

Therefore, a method that quantitatively determines the Sn redox profile of float glass using equipment commonly used in laboratories is required. The wet chemical analysis method is suitable for this purpose because it can be performed daily in the laboratory with relatively high precision, low detection limits, and low costs. It can also achieve fine depth resolution when combined with an etching technique. This study proposes and demonstrates a novel wet chemical analysis method for determining the Sn redox profile from the tin side of the float glass.

The challenges of wet chemical analysis include maintaining the balance of the target ions (Sn^{2+} and Sn^{4+}), separately identifying their concentrations, and determining their depth profiles. Regarding the first and second challenges, we have already established a method to determine the concentration of Sn^{2+} and Sn^{4+} in a bulk glass that contains Fe_2O_3[26]. In this method, a mixture of ascorbic acid, hydrochloric acid, and hydrofluoric acid was used to decompose the ground glass sample in a vessel with nitrogen flow. The ascorbic acid reduced Fe^{3+}, thus preventing the redox reaction between Fe^{3+} and Sn^{2+} in the etchant[26]. After etching, the HF in the etchant was masked with boric acid to ensure safety[27,28]. The etchant was sampled and Sn^{2+} in the etchant was extracted as a

diethyldithiocarbamate complex[29]. Inductively coupled plasma atomic emission spectroscopy was used to determine the concentrations of Sn^{4+} and total Sn in the aqueous phase, from which the concentration of Sn^{2+} can be calculated. However, it is a challenge to precisely determine the Sn redox depth profile from the tin side of the float glass as this method was used for bulk glass analysis. To overcome the challenge, in this paper, we propose a new method that combines the tin speciation method[26] and a stepwise etching technique that was previously used to determine the concentrations of ferrous and total iron on the atmosphere-side surface of float glass[30]. This etching technique was conducted with CYTOP® masking, a thermoplastic perfluoropolymer that had water-repellency and resistance to the etchant, to etch a selected surface of glass. In our proposed method, the tin side of a float glass was etched stepwise under nitrogen flow with a hydrofluoric acid (HF) etchant containing ascorbic acid. The depth profiles of Sn^{4+} and total Sn in the surface region of the tin side were precisely determined utilizing the previous method[26], and the profiles of Sn^{2+} and Sn redox were calculated. Below, we compare and discuss the profiles of each valence of Sn and Sn redox with those in previous studies.

4.2   Experimental

4.2.1   Glass materials

  Commercial soda lime silicate glass of 3.2 mm thickness produced by AGC Inc. using a float process was used. Its approximate composition is $71SiO_2–13Na_2O–9CaO–5MgO–2Al_2O_3$ (mass%). As minor components, it contains 0.5 mass% Fe_2O_3 and 0.2 mass% SO_3. Its density is 2.50 g/cm^3.

4.2.2   Apparatus and instrumentation

  An ultrasonic cleaner (VS-100III; AS ONE, Osaka, Japan) was used at a frequency of 28 kHz for the etching. A 10 mL syringe (Terumo Corporation, Tokyo, Japan) and a syringe filter with a 0.45 μm pore

(Toyo Roshi Kaisya, Ltd., Tokyo, Japan) were used to transfer the sample solutions and remove any

unexpected solids. A 100 mL glass separatory funnel was used to extract Sn^{2+} into the organic phase.

A polyimide tape (Kapton® film adhesive tape 650S #50, TERAOKA, Tokyo, Japan) was used to

mask the glass. An inductively coupled plasma atomic emission spectrometer (SPS5520, Hitachi High-

Tech Corporation, Tokyo, Japan) was used to determine Sn and Si concentrations.

4.2.3 Reagents and chemicals

Hydrofluoric acid (50 mass%) and hydrochloric acid (36 mass%), both of atomic absorption

spectrometry grade, boric acid, ascorbic acid, and mixed xylene, all of special grade, and standard

solutions of Sn and Si (1 g/L) of ion-chromatography grade were obtained from Kanto Chemical Co.,

Inc., Tokyo, Japan. Diethylammonium diethyldithiocarbamate of Wako 1st grade was obtained from

FUJIFILM Wako Pure Chemical Corporation, Osaka, Japan. CYTOP® solution from CTL-809M,

AGC Inc., Tokyo, Japan was used to mask the glass. Deionized water was degassed before use.

4.2.4 Procedures

4.2.4.1 Etching procedure

The glass was cut into pieces of size 4×4 cm^2. Surfaces other than the tin side were coated with

CYTOP® in accordance with a previous study[30]. Fig. 4-1 shows a schematic representation of the

experimental setup used for etching the glass sample. The sample was placed in a polyethylene bag

and 1 mL of 5 mass% ascorbic acid and 10 mL of a mixture of HF (1.4 mol/L) and HCl (0.12 mol/L),

referred to as the etchant, was added. The polyethylene bag containing the sample and etchant was

placed in a glass beaker filled with tap water. A glass bell with nitrogen flowing through it was used

to maintain an inert atmosphere so as to prevent oxidation of Sn^{2+}. The etching procedure was

performed using ultrasonication at 28 kHz for 2–4 min depending on the required etching depth.
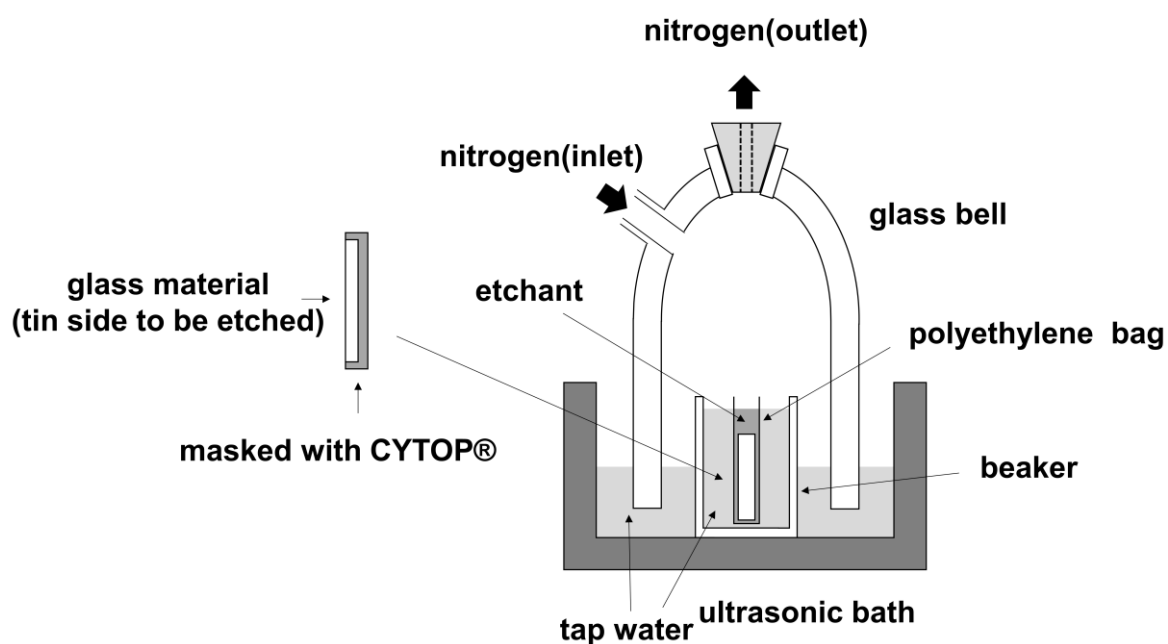
Fig. 4-1 Schematic representation of the experimental setup for etching of the glass sample. The sample is etched in the polyethylene bag with ultrasonication at 28 kHz under nitrogen flow.

4.2.4.2　Separation of Sn^{2+}

After etching, the glass bell was removed and the etchant in the polythene bag was transferred to a 30 mL polypropylene cup. Boric acid solution (5 mL, 4 mass%) was added to the polyethylene bag to wash the sample surface and mask the hydrofluoric acid[27,28], and the washings were transferred to the same polypropylene cup. This washing procedure was repeated twice, and performed quickly to prevent oxidation of the Sn^{2+}. The sample solution in the cup was mixed thoroughly and diluted to the mark of 30 mL with water. This solution was named "solution A." Two approximately 10 mL samples of of solution A were taken, using a syringe, and the 20 mL of solution A was transferred with a syringe into a 100 mL glass separatory funnel containing 5 mL of xylene containing 0.1 mass%

91

diethylammonium diethyldithiocarbamate. A syringe filter was used to remove any unexpected solids. The funnel was shaken for 1 min to extract Sn^{2+} from solution A into the organic phase. The extraction procedure was repeated twice. The water phase in the funnel was sampled and this solution was named "solution B."

4.2.4.3 Determination of Sn and Si

The concentrations of Sn present in solutions A and B, which contain total Sn and Sn^{4+}, respectively, and the concentration of Si present in solution A were determined by ICP-AES. Table 1 lists the measurement conditions.

Table 1 ICP-AES measurement conditions

RF power	1.2 kW
Plasma gas flow	15.0 L/min
Auxiliary gas flow	1.5 L/min
Nebulizer gas pressure	0.75 MPa
Emission line	Sn(II) : 189.927 nm
	Si(I) : 251.612 nm

4.2.4.4 Calculation of the etching depth and Sn concentration

The etching depth was calculated using the Si concentration determined using Equation 1. In a previous study, it was confirmed[30] that the calculated depth agreed well with the depth measured using a stylus surface profiler. The concentrations of total Sn, Sn^{4+}, and Sn^{2+} at each depth were calculated using Equations 2, 3, and 4, respectively. The concentrations were calculated as SnO_2

92

mass% following the conventions for describing the composition of oxide glass. The factor 2.14 in

Equation 4-1 represents the conversion factor from Si to SiO_2. Similarly, the factor 1.27 in Equations

4-2 and 4-3 is the conversion factor from Sn to SnO_2. In this study, the ratio of Sn^{2+} to total Sn is

defined as Sn redox, and indicates the degree of reduction, as shown in Equation 4-5.

$$\text{Etching depth (μm)} = \frac{\text{Si in solution A} \left(\frac{\text{μg}}{\text{mL}}\right) \times 30 \text{ (mL)} \times 2.14}{\text{Area of sample (cm}^2) \times 2.50 \left(\frac{\text{g}}{\text{cm}^3}\right) \times 71 \text{ (SiO}_2 \text{ mass%)}} \tag{4-1}$$

$$\text{Total Sn (as SnO}_2 \text{ mass%)} = \frac{\text{Sn in solution A} \left(\frac{\text{μg}}{\text{mL}}\right) \times 30 \text{ (mL)} \times 1.27}{\text{Area of sample (cm}^2) \times 2.50 \left(\frac{\text{g}}{\text{cm}^3}\right) \times \text{Etching depth (μm)}} \tag{4-2}$$

$$\text{Sn}^{4+} \text{ (as SnO}_2 \text{ mass%)} = \frac{\text{Sn in solution B} \left(\frac{\text{μg}}{\text{mL}}\right) \times 30 \text{ (mL)} \times 1.27}{\text{Area of sample (cm}^2) \times 2.50 \left(\frac{\text{g}}{\text{cm}^3}\right) \times \text{Etching depth (μm)}} \tag{4-3}$$

$$\text{Sn}^{2+} \text{ (as SnO}_2 \text{ mass%)} = \text{Total Sn (as SnO}_2 \text{ mass%)} - \text{Sn}^{4+} \text{ (as SnO}_2 \text{ mass%)} \tag{4-4}$$

$$\text{Sn redox (%)} = \frac{\text{Sn}^{2+} \text{ (as SnO}_2 \text{ mass%)}}{\text{Total Sn (as SnO}_2 \text{ mass%)}} \times 100 \tag{4-5}$$

4.2.4.5　Blank test

A blank test was performed throughout the entire procedure comprising etching, separation, and

determination. The test was repeated four times to determine the mean blank values and their standard

deviations (σ). The limit of quantification was defined as the mean blank value plus 10σ.

4.3　　　Results

Fig. 4-2 shows (a) the concentration of total Sn, Sn^{2+}, and Sn^{4+}, and (b) Sn redox, as a function of the depth from the tin side, where the middle point of each etching step is regarded as the depth. The total Sn concentration was approximately 1.4 mass% at the outermost surface. It decreased steeply from the outermost surface and showed a buried peak at a depth of 7–8 μm below the surface. The peak is the so-called tin hump, and its concentration was approximately 0.6 mass%. The total Sn concentration decreased gently in the part deeper than the tin hump and was less than 0.05 mass% (as SnO_2) at a depth of 17 μm. The Sn^{2+} concentration simply decreased from the surface and showed no buried peak. The Sn^{4+} concentration showed a complicated profile, with the first peak at the outermost surface(discussed in the next section) and the second peak at a depth of 7–8 μm, consistent with the depth of the tin hump.

The Sn redox profile calculated from these results had a value of 53 % on the outermost surface, which subsequently increased to a maximum of 75 % at a depth of 1.5 μm, gradually decreased to 51 % at 6 μm, and then decreased sharply to 13 % at a depth of 7–8 μm. This depth is consistent with the depth of the tin hump. In the deeper parts of the tin hump, Sn redox gradually decreased to less than 10 %. The part shallower than the tin hump was the so-called reduced layer, and the part deeper than the tin hump was the so-called oxidized layer.

Three days were required to complete all the analyses, including sample preparation, etching, Sn^{2+} separation, and ICP-AES measurements. The ICP-AES analysis can be performed in the following days owing to the stable nature of the solutions.

From the blank test, the limits of quantification for total Sn and Sn^{4+} were both 0.02 mass% (as SnO_2) when 16 cm^2 (4 cm × 4 cm) of glass was etched to a depth of 1 μm.
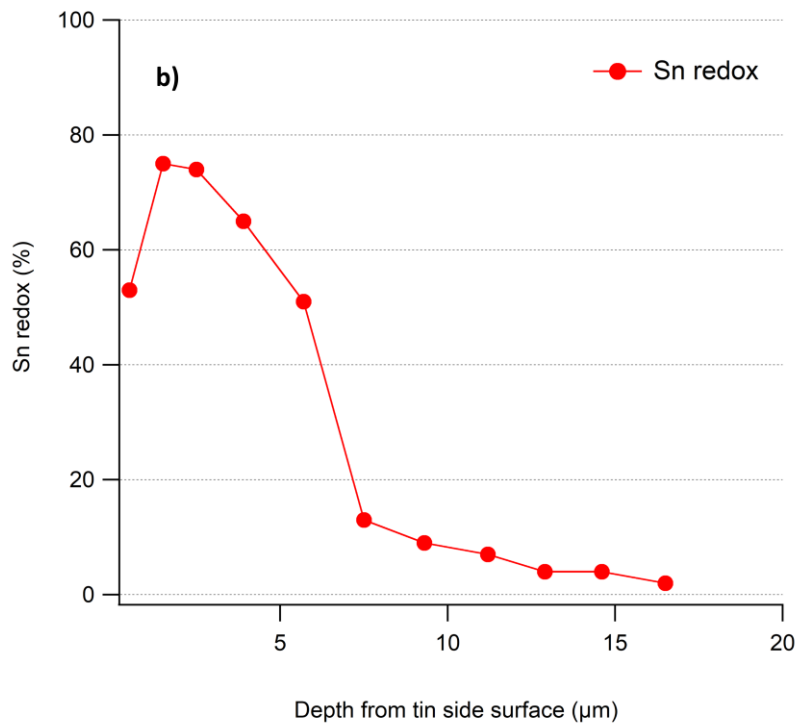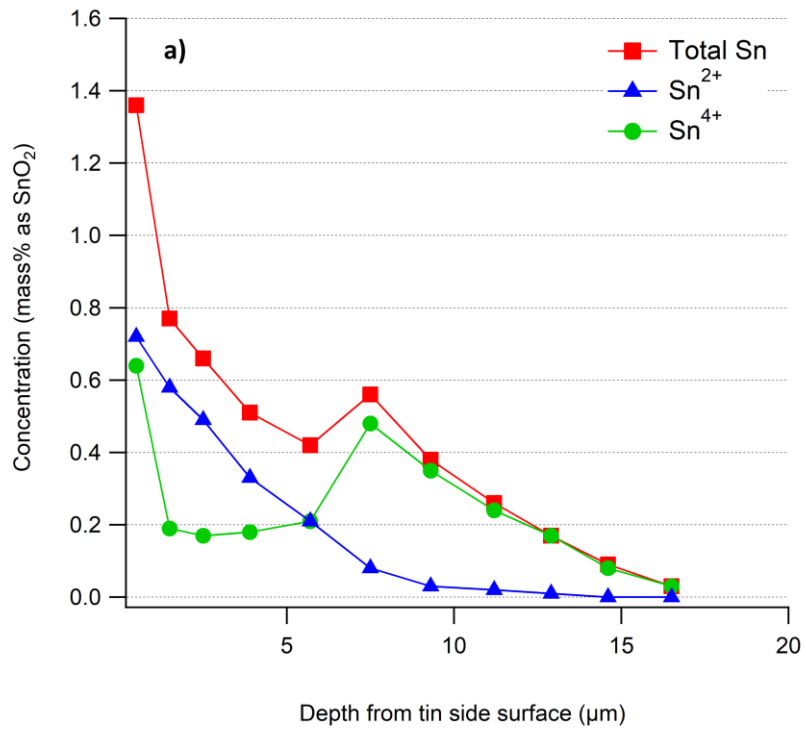
Fig. 4-2 a) Concentration of total Sn, Sn²⁺, and Sn⁴⁺; b) Sn redox, as a function of depth from the tin side

4.4   Discussion

The method proposed in this study determines the concentrations of total Sn and Sn^{4+} on the tin side of the float glass in the depth direction. It also allows the calculation of Sn^{2+} and Sn redox. The etching depth can be varied with the etching time. From the limit of quantification, the minimum etching depth (= depth resolution) can be 0.1 μm when the total Sn concentration (as SnO_2) is greater than 0.2 mass%. The depth corresponding to the SnO_2 concentration was approximately 12 μm from the tin side surface for the sample used in this study. This depth is sufficient for a detailed study because it is deeper than the depth of the tin hump.

It is clear that the proposed method is the most quantitative compared to the existing methods (TMS, CEMS, and XAFS) because these methods are virtually unquantifiable, as mentioned in the introduction. Furthermore, when the total Sn concentration (as SnO_2) is greater than 0.2 mass%, the proposed method has the excellent depth resolution of 0.1 μm, considerably smaller than that of conventionally used methods such as XAFS, which has obtained the previous best depth resolution of 1 μm. The analysis time required by the proposed method, three days for one sample, is reasonable compared to that of the existing methods: XAFS involves the use of synchrotron radiation facilities, which requires time to conduct the experiment, and TMS and CEMS also involve time-consuming measurements. Finally, the proposed method can be implemented in the laboratory because it uses only commonly used apparatus and equipment.

The outermost Sn^{4+} peak is attributed to the low-temperature oxidation of Sn^{2+} penetrating during the float process when the glass encounters an oxidizing atmosphere upon leaving the float chamber[11,17,20]. In the region shallower than the tin hump, Sn^{2+} was the majority; however, in the deeper part of the tin hump, Sn^{4+} was predominant. This is consistent with previous studies[13–17,19,20,23] and supports the diffusion-redox mechanism. In contrast, this study revealed that a certain amount of Sn^{4+} was present in an area shallower than the tin hump. Johnson et al. [19] confirmed the

same results, but there was no clear explanation. This can be explained when the penetration speed of Sn^{2+} is higher than the rate at which glass is reduced from the surface by the reducing float atmosphere, as shown in a previous simulation[31]. In other words, Sn^{4+} can be produced by oxidation of the penetrating Sn^{2+} by the polyvalent elements (Fe^{3+} and S^{6+}) in the glass that existed before the depth at which the tin hump could finally be formed. This study also quantitatively revealed that approximately 90 % of the total Sn was Sn^{4+} in the deeper part of the tin hump.

Although we revealed the detailed Sn profile on the tin side of the float glass with high quantitative and depth resolution, the profile is generally complicated and affected by many factors, including the atmosphere in the bath (including oxygen concentration), the thickness of the glass (float bath residence time, stretching, or compression effect), the concentrations of polyvalent elements in the glass, and the diffusion coefficients of Sn^{2+} and Sn^{4+} at each temperature. Therefore, although it has become possible to have a new quantitative discussion divided into Sn^{2+} and Sn^{4+} in this study, it is still not sufficient to fully understand the profile of Sn on the tin side of float glass. To better understand the Sn profile, it is necessary to develop a new quantitative valence analysis method for Fe and S in the depth direction of the glass and reflect the information in the simulation.

4.5   Conclusions

This study investigated a novel wet chemical analysis method for determining the depth profile of total Sn and Sn^{4+} ions from the tin side of float glass. The method entails stepwise etching of a glass sample, separation of tin species, and determination of the Sn^{4+} and total Sn concentrations. The Sn^{2+} concentration was calculated using the total Sn and Sn^{4+} concentrations, and the ratio of Sn^{2+} to total Sn (the Sn redox) was calculated. The float glass sample was etched with a mixture of ascorbic acid, hydrochloric acid, and hydrofluoric acid under a nitrogen purge. Sn^{2+} was separated from the etchant into an organic phase as a diethyldithiocarbamate complex. Inductively coupled plasma atomic emission spectroscopy was used to determine the concentrations of total Sn and Sn^{4+}. It was also used to determine the Si concentration in the etchant and calculate the etching depth. This method provides quantitative concentration profiles of total Sn, Sn^{4+}, Sn^{2+}, and Sn redox in the depth direction. The results showed that the region of the sample shallower than the tin hump constituted the reduced layer and the part deeper than the tin hump was the oxidized layer. In addition, the outermost surface was oxidized even though it was inside the reduced layer. These results are consistent with those of the previous studies. Furthermore, our results revealed a complicated Sn^{4+} concentration profile, consisting of a first peak at the outermost surface and a second peak at a depth of 7–8 μm, which is consistent with the depth of the tin hump. In contrast, the Sn^{2+} concentration decreased from the surface and exhibited no buried peaks. The proposed method has the finest depth resolution, 0.1 μm, when the total Sn concentration (as SnO_2) is greater than 0.2 mass%, a resolution superior to that of the existing methods. It can be easily implemented in the laboratory because it uses only commonly used apparatus and equipment. This study provides detailed information on the penetration of Sn into the tin side of float glass, and the proposed method strongly contributes to the float process for producing high-quality glass.

4.6   References

[1]   L.A.B. Pilkington, The float glass process, Proceedings of the Royal Society of London. Series A, Mathematical and Physical Sciences. 314 (1969) 1–25. https://doi.org/10.1098/rspa.1969.0212.

[2]   T. Kloss, G. Lautenschlaeger, K. Schneider, Advances in the process of floating borosilicate glasses and some recent applications for specialty borosilicate float glasses, Glass Technology. 41 (2000) 177–181.

[3]   K. Maeda, Glass Substrate for Flat Panel Displays, Journal of the Japan Society for Precision Engineering. 70 (2004) 466–469. https://doi.org/10.2493/jjspe.70.466.

[4]   Y. Arai, M. Inoue, K. Ishikawa, T. Yokote, Y. Kondo, K. Mori, Evolution of the glass light guide plate and its peripheral technologies for large size TV application, 2017. https://doi.org/10.1002/sdtp.11964.

[5]   K. Hayashi, J. Endo, S. Akiba, T. Nakashima, Novel damage-resistant glass for display cover, in: Proceedings of the International Display Workshops, 2011.

[6]   J.S. Sieger, Chemical characteristics of float glass surfaces, Journal of Non-Crystalline Solids. 19 (1975) 213–220. https://doi.org/10.1016/0022-3093(75)90086-1.

[7]   Y. Hayashi, Y. Fukuda, M. Kudo, Investigation on changes in surface composition of float glass-mechanisms and effects on the mechanical properties, Surface Sciences. 507–510 (2002) 872–876. www.elsevier.com/locate/susc.

[8]   Y. Hayashi, K. Matsumoto, M. Kudo, Mechanisms and chemical effects of surface tin enrichment on float glass, Glass Technology. 42 (2001) 130–133. https://www.scopus.com/inward/record.uri?eid=2-s2.0-0035435574&partnerID=40&md5=8bbc48e04a12d30b83cdd0addf68f9ed (accessed January 19, 2022).

[9]   Y. Hayashi, R. Akiyama, M. Kudo, Surface characterization of float glass related to changes in the optical properties after reheating, Surface and Interface Analysis. 31 (2001) 87–92. https://doi.org/10.1002/sia.960.

[10]   G.H. Frischat, Tin ions in float glass cause anomalies, Comptes Rendus Chimie. 5 (2002) 759–763. https://doi.org/10.1016/S1631-0748(02)01436-4.

[11]   K.F.E. Williams, M.F. Thomas, J. Greengrass, J.M. Bradshaw, Effect of tin on some physical properties of the bottom surface of float glass and the origin of bloom, Glass Technology. 40 (1999) 103–107.

[12]   S. Takeda, Oxygen and silver diffusion into float glass, Journal of Non-Crystalline Solids. 352 (2006) 3910–3913. https://doi.org/10.1016/j.jnoncrysol.2006.06.010.

[13]   Y. Hayashi, K. Matsumoto, M. Kudo, The diffusion mechanism of tin into glass governed by redox reactions during the float process, Journal of Non-Crystalline Solids. 282 (2001) 188–196. https://doi.org/10.1016/S0022-3093(01)00319-2.

[14]   G.H. Frischat, C. Müller-Fildebrandt, D. Moseler, G. Heide, On the origin of the tin hump in several float glasses, Journal of Non-Crystalline Solids. 283 (2001) 246–249. https://doi.org/10.1016/S0022-3093(01)00491-4.

[15]   W. Meisel, Depth profile of tin in float glass - a CEMS study, Glass Science and Technology: Glastechnische Berichte. 72 (1999) 291–294.

[16]   A.M. Flank, P. Lagarde, J. Jupille, H. Montigaud, Redox profile of the glass surface, Journal of Non-Crystalline Solids. 357 (2011) 3200–3206. https://doi.org/10.1016/j.jnoncrysol.2011.03.046.

[17]   Y. Hayashi, K. Matsumoto, M. Kudo, The Diffusion Mechanism of Tin into Glass during the Float Process, Hyomen Kagaku. 22 (2001) 412–418. https://doi.org/10.1380/jsssj.22.412.

[18]   A. Kumar, S.P. Singh, R. Pyare, Sn^{2+}-Sn^{4+} and Fe^{2+}-Fe^{3+} redox interaction in $30Na_2O$-$70SiO_2$

glass, Glastechnische Berichte. 64 (1991) 106–108. http://www.bl.uk/reshelp/atyourdesk/docsupply/help/terms/index.html.

[19] K.F.E. Williams, C.E. Johnson, B.P. Tilley, D. Gelder, J.A. Johnson, Tin oxidation state, depth profiles of Sn^{2+} and Sn^{4+} and oxygen diffusivity in float glass by Mössbauer spectroscopy, Journal of Non-Crystalline Solids. 211 (1997) 164–172. https://doi.org/10.1016/S0022-3093(96)00636-9.

[20] K.F.E. Williams, C.E. Johnson, O. Nikolov, M.F. Thomas, J.A. Johnson, J. Greengrass, Characterization of tin at the surface of float glass, Journal of Non-Crystalline Solids. 242 (1998) 183–188. https://doi.org/10.1016/S0022-3093(98)00799-6.

[21] W.E. Baitinger, P.W. French, E.L. Swarts, Characterization of tin in the bottom surface of float glass by ellipsometry and XPS, Journal of Non-Crystalline Solids. 38–39 (1980) 749–754.

[22] P.D. Townsend, N. Can, J. Chandler, B.W. Farmery, R. Lopez-Heredero, A. Peto, L. Salvin, D. Underdown, B. Yang, Comparisons of tin depth profile analyses in float glass, Journal of Non-Crystalline Solids. 223 (1998) 73–85. https://doi.org/10.1016/S0022-3093(97)00348-7.

[23] J. A. Johnson, C. E. Johnson, K. F. E. Williams, D. Holland, M. M. Karim, Mössbauer spectra of tin in float glass, Hyperfine Interactions. 95 (1995) 41–51.

[24] G. Principi, A. Maddalena, A. Gupta, F. Geotti-Bianchini, S. Hreglich, M. Veritá, Oxidation state of surface tin in an industrially produced float glass, Nuclear Inst. and Methods in Physics Research, B. 76 (1993) 215–217. https://doi.org/10.1016/0168-583X(93)95185-8.

[25] J.A. Johnson, C.E. Johnson, Mössbauer spectroscopy as a probe of silicate glasses, Journal of Physics Condensed Matter. 17 (2005) R381–R412. https://doi.org/10.1088/0953-8984/17/8/R01.

[26] Y. Saijo, M. Murata, T. Kajihara, H. Hijiya, Y. Suzuki, R. Akiyama, M. Shimizu, Y. Shimotsuma, K. Miura, Speciation of tin ions in oxide glass containing iron oxide through

solvent extraction and inductively coupled plasma atomic emission spectrometry after the decomposition utilizing ascorbic acid, Analytical Sciences. 38 (2022) 881–888. https://doi.org/10.1007/s44211-022-00110-w.

[27]   B. Bernas, A New Method for Decomposition and Comprehensive Analysis of Silicates by Atomic Absorption Spectrometry, Analytical Chemistry. 40 (1968) 1682–1686. https://doi.org/10.1021/ac60267a017.

[28]   D.E. Buckley, R.E. Cranston, Atomic absorption analyses of 18 elements from a single decomposition of aluminosilicate, Chemical Geology. 7 (1971) 273–284. https://doi.org/10.1016/0009-2541(71)90012-X.

[29]   P.F. Wyatt, Diethylammonium Diethyldithiocarbamate for the Separation and Determination of Small Amounts of Metals Part II. The Isolation and Determination of Arsenic, Antimony and Tin in Organic Compounds, Analyst. 80 (1955) 368–379.

[30]   R. Akiyama, N. Kanno, Y. Suzuki, K. Yamamoto, Determination of ferrous and total iron at the surface of float glass by spectrophotometry combined with a stepwise etching technique, Glass Technology - European Journal of Glass Science and Technology Part A. 56 (2015) 37–42.

[31]   Q. Zhang, Z. Chen, Z. Li, Simulation of tin penetration in the float glass process (float glass tin penetration), Applied Thermal Engineering. 31 (2011) 1272–1278. https://doi.org/10.1016/j.applthermaleng.2010.12.030.

Publication List

Chapter1

'Determination of sulfur in soda-lime silicate glass by inductively coupled plasma atomic emission spectroscopy following separation using an alumina column',

Yoshitaka Saijo, Yuichi Suzuki, Ryoji Akiyama and Kiyotaka Miura,

Journal of the Ceramic Society of Japan, **129** [1] 54-59 (2021)

https://doi.org/10.2109/jcersj2.20185

Chapter2

'Separation and Determination of Sulfide Sulfur and Sulfate Sulfur in Soda Lime Silicate Glass',

Yoshitaka Saijo, Yuichi Suzuki, Makiko Murata, Ryoji Akiyama, Masahiro Shimizu, Yasuhiko Shimotsuma, Kiyotaka Miura,

Journal of Non-Crystalline Solids, **571**, 121072 (2021).

https://doi.org/10.1016/j.jnoncrysol.2021.121072

Chapter3

'Speciation of tin ions in oxide glass containing iron oxide through solvent extraction and inductively coupled plasma atomic emission spectrometry after the decomposition utilizing ascorbic acid'

Yoshitaka Saijo, Makiko Murata, Takato Kajihara, Hiroyuki Hijiya, Yuichi Suzuki, Ryoji Akiyama, Masahiro Shimizu, Yasuhiko Shimotsuma, Kiyotaka Miura,

Analytical Sciences, **38**, 881-888 (2022)

https://doi.org/10.1007/s44211-022-00110-w

Chapter4

'Speciation Analysis of Tin at the Tin Side of Float Glass by Solvent Extraction Combined with a Stepwise Etching Technique'

Yoshitaka Saijo, Yuichi Suzuki, Ryoji Akiyama, Masahiro Shimizu, Yasuhiko Shimotsuma, and Kiyotaka Miura,

Acknowledgements

Copyright and Sources

Chapter 1

The content of Chapter 1 was reproduced from [Journal of the Ceramic Society of Japan, **129**, 54-59 (2021)]. The journal contents may be reproduced without permission.

Chapter 2

The content of Chapter 2 was reproduced from [Journal of Non-Crystalline Solids, **571**, 121072 (2021)] with permission of Elsevier.

Chapter 3

The content of Chapter 3 was reproduced from [Analytical Sciences, **38**, 881-888 (2022)] with permission of Springer Nature.

Chapter 4

The content of Chapter 4 was reproduced from [Journal of Non-Crystalline Solids, **592**, 121752 (2022)] with permission of Elsevier.